for QCD Critical Point

Rajiv V. Gavai
T. I. F. R., Mumbai, India

Importance of Being Critical

Lattice QCD Results

Searching Experimentally

Summary

Importance of Being Critical

Phase Diagram of Water

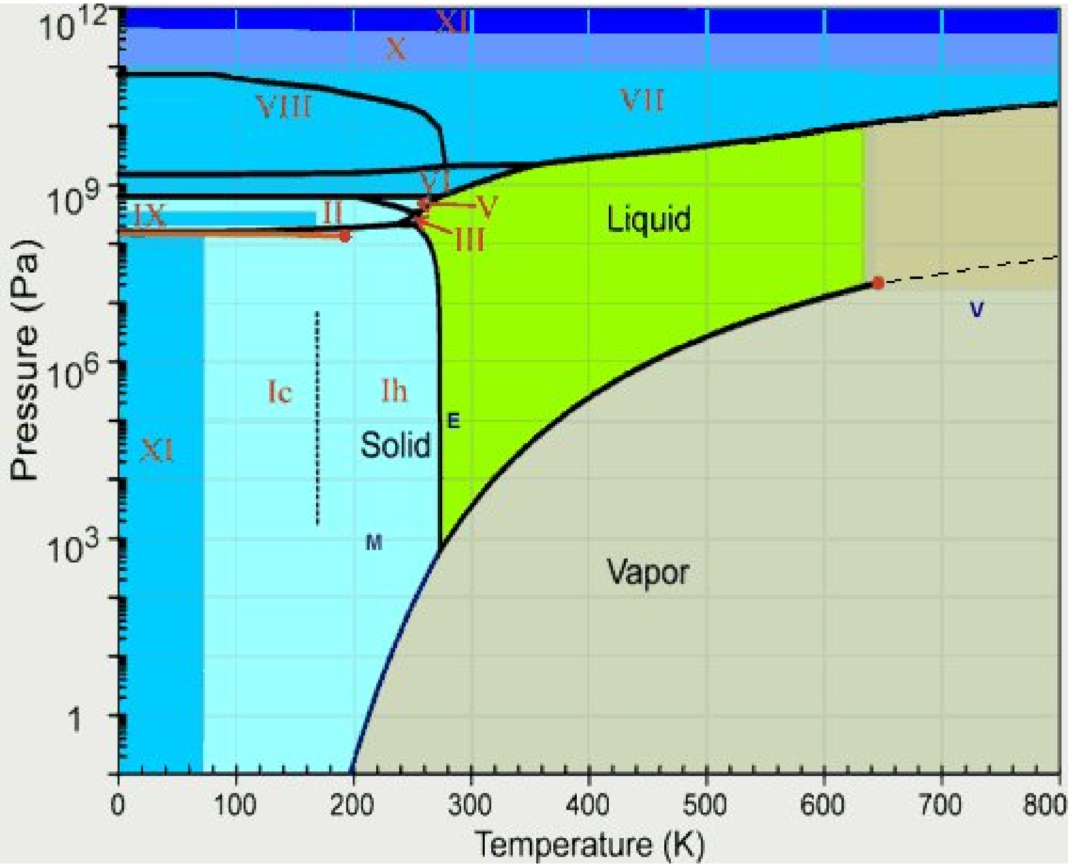

Importance of Being Critical

Phase Diagram of Water

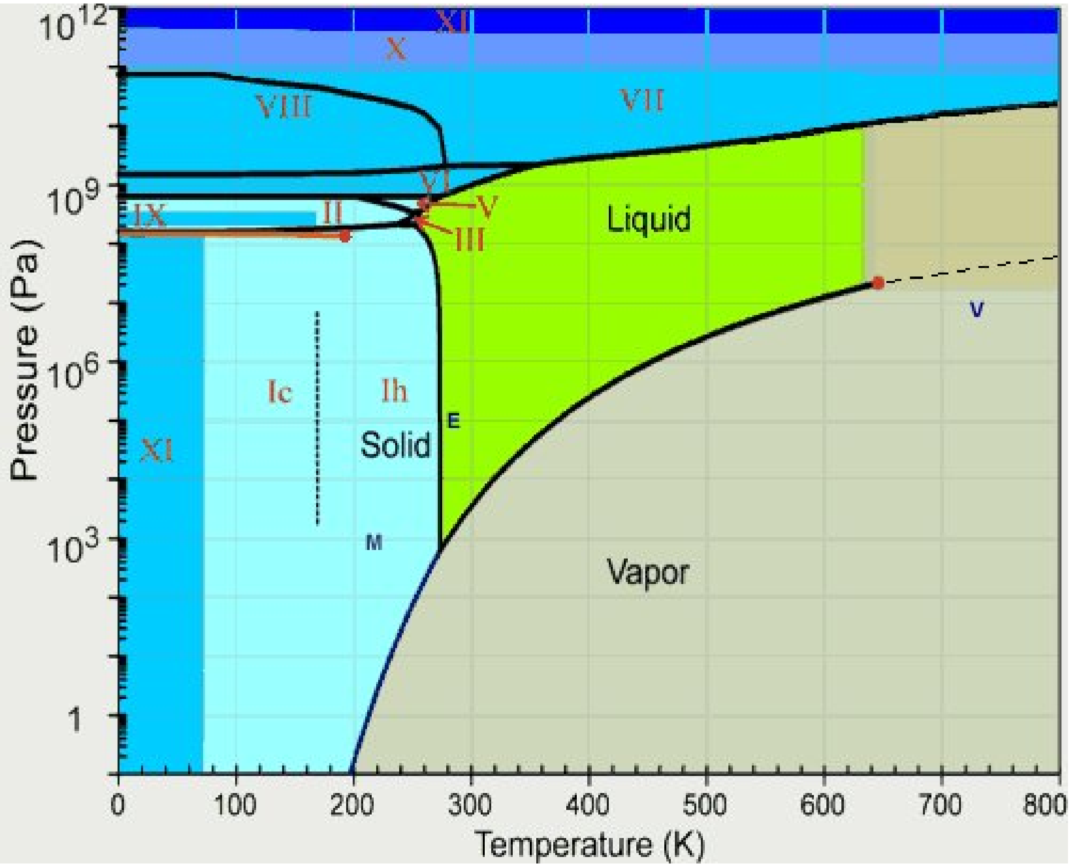

- One, possibly two, critical points
- Extreme density fluctuations $\Longrightarrow$ Critical Opalescence

Importance of Being Critical

Phase Diagram of Water

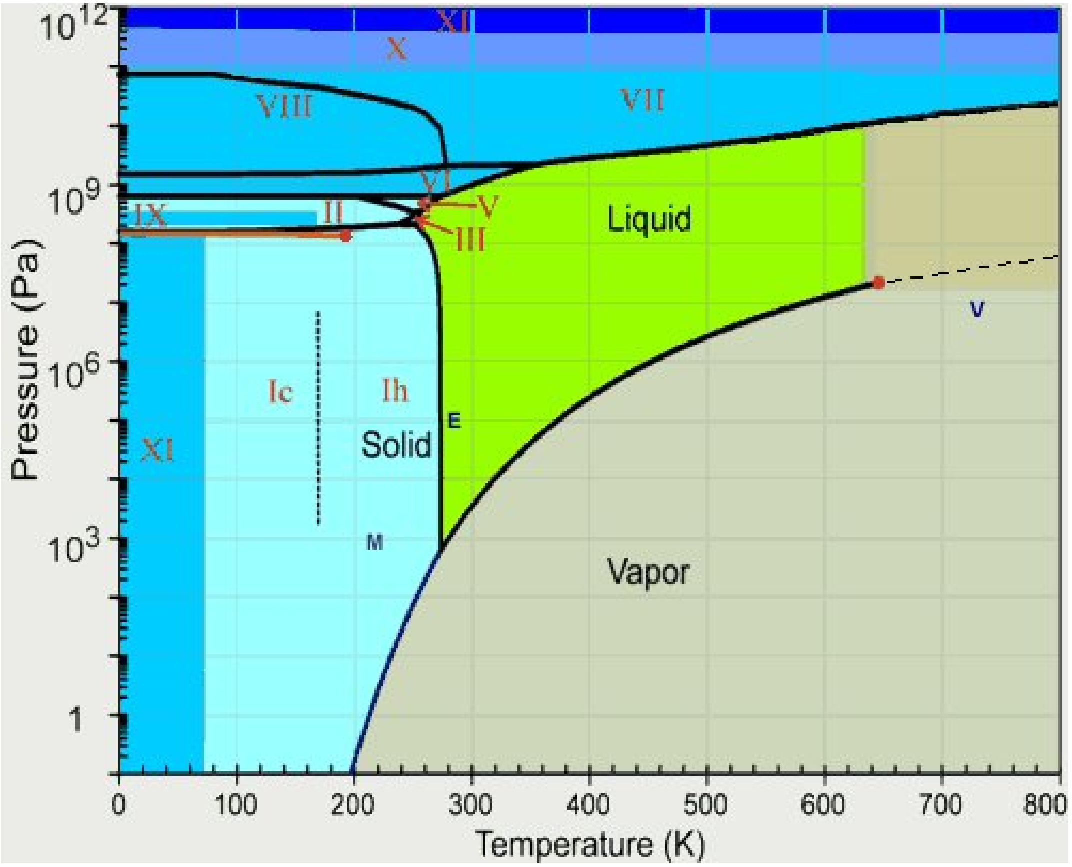

- One, possibly two, critical points
- Extreme density fluctuations $\Longrightarrow$ Critical Opalescence
- Dielectric constant & Viscosity $\downarrow$.
- Many liquid fueled engines exploit such supercritical transitions.

FIRST ORDER **SECOND ORDER**

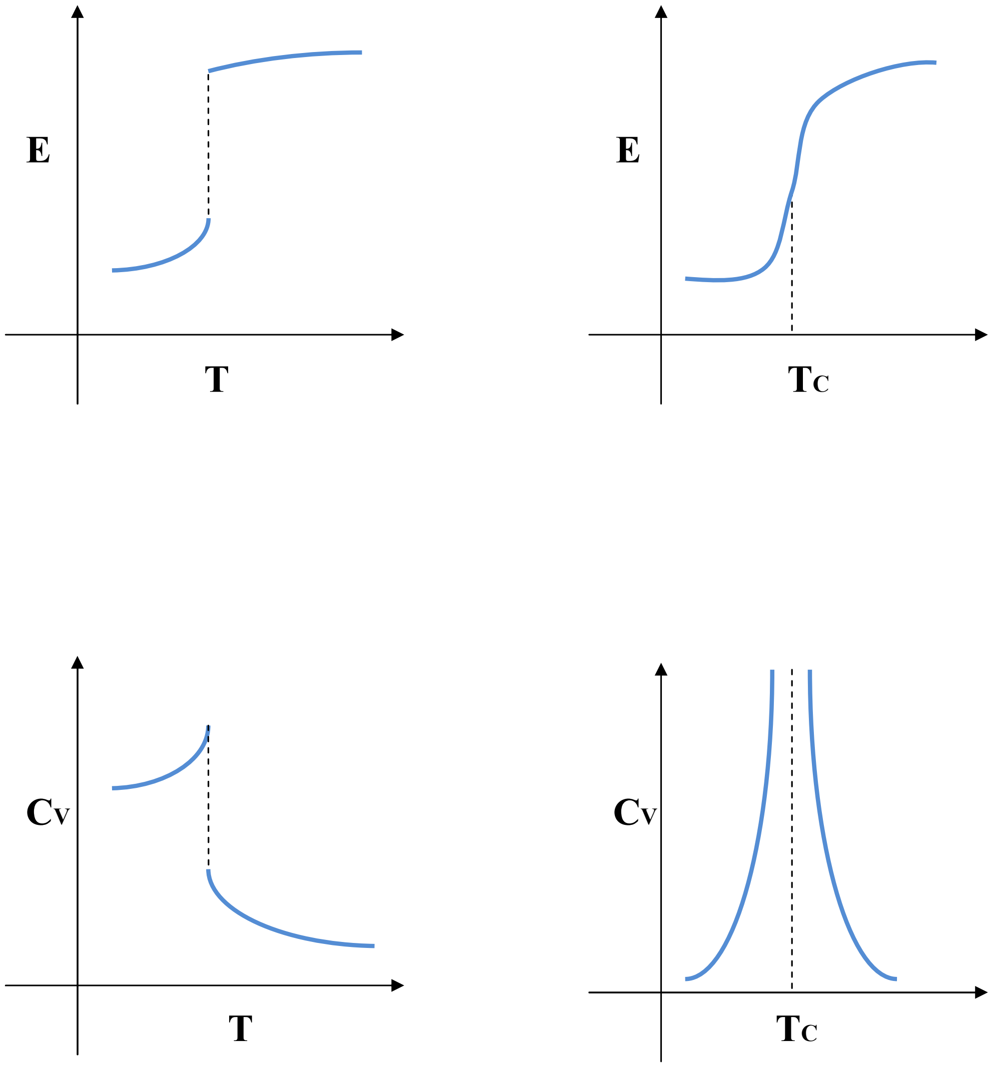

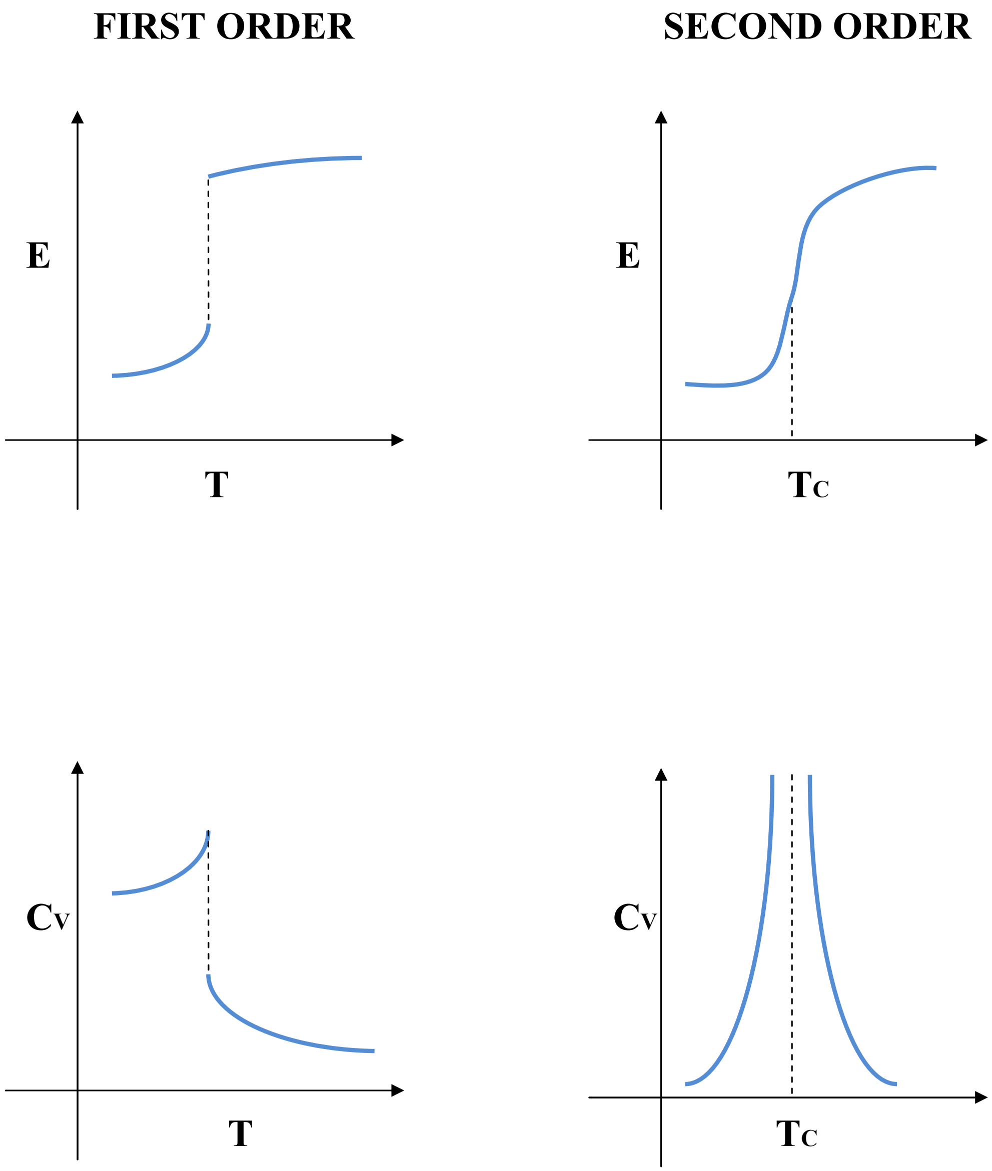

- Discontinuous ϵ – Nonzero Latent Heat– & finite C_v $\rightarrow$ First order PT.

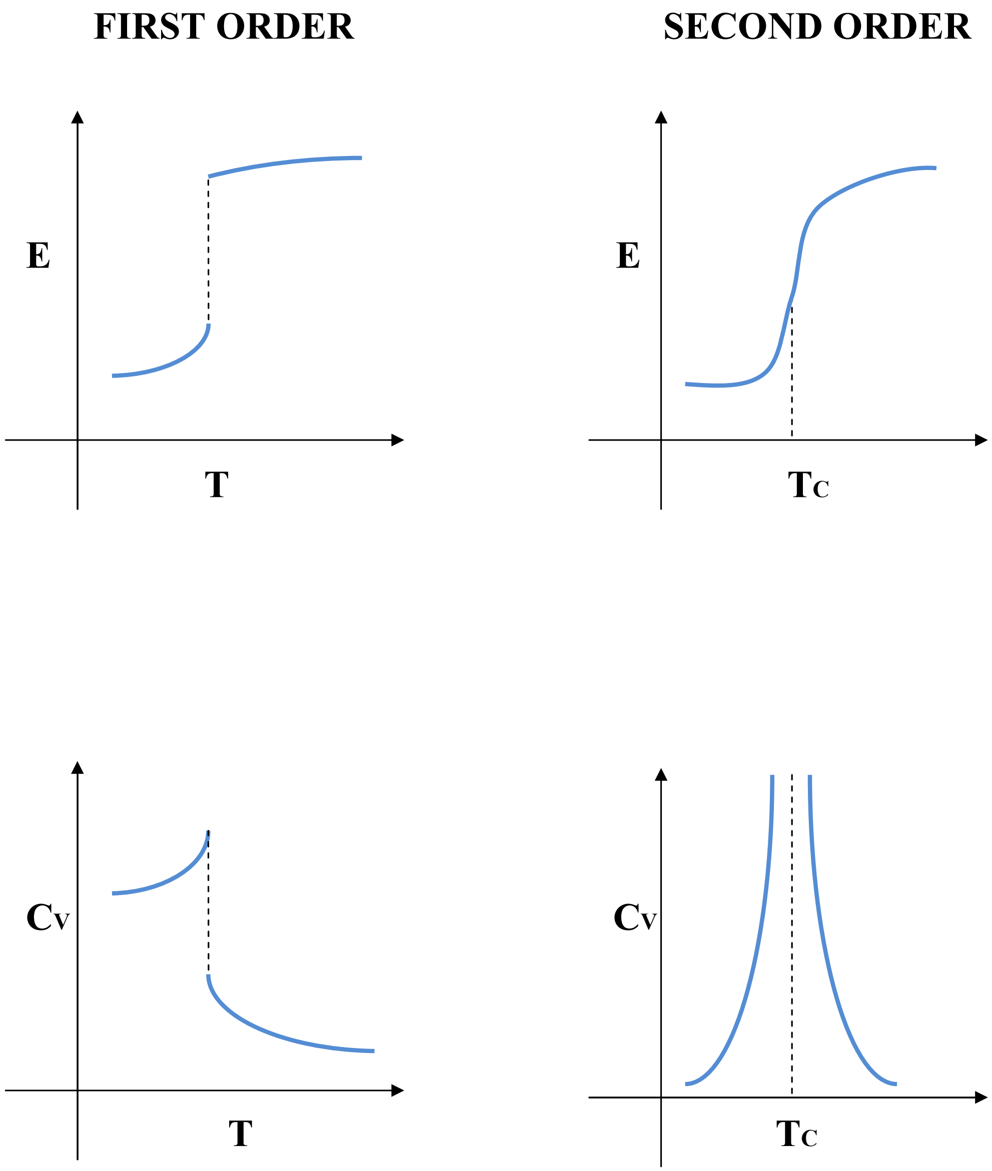

- Discontinuous ϵ – Nonzero Latent Heat– & finite C_v $\rightarrow$ First order PT.

- Continuous ϵ, & diverging C_v $\rightarrow$ Second order PT.

- In(Finite) Correleation Length at 2nd (1st) Order transition.

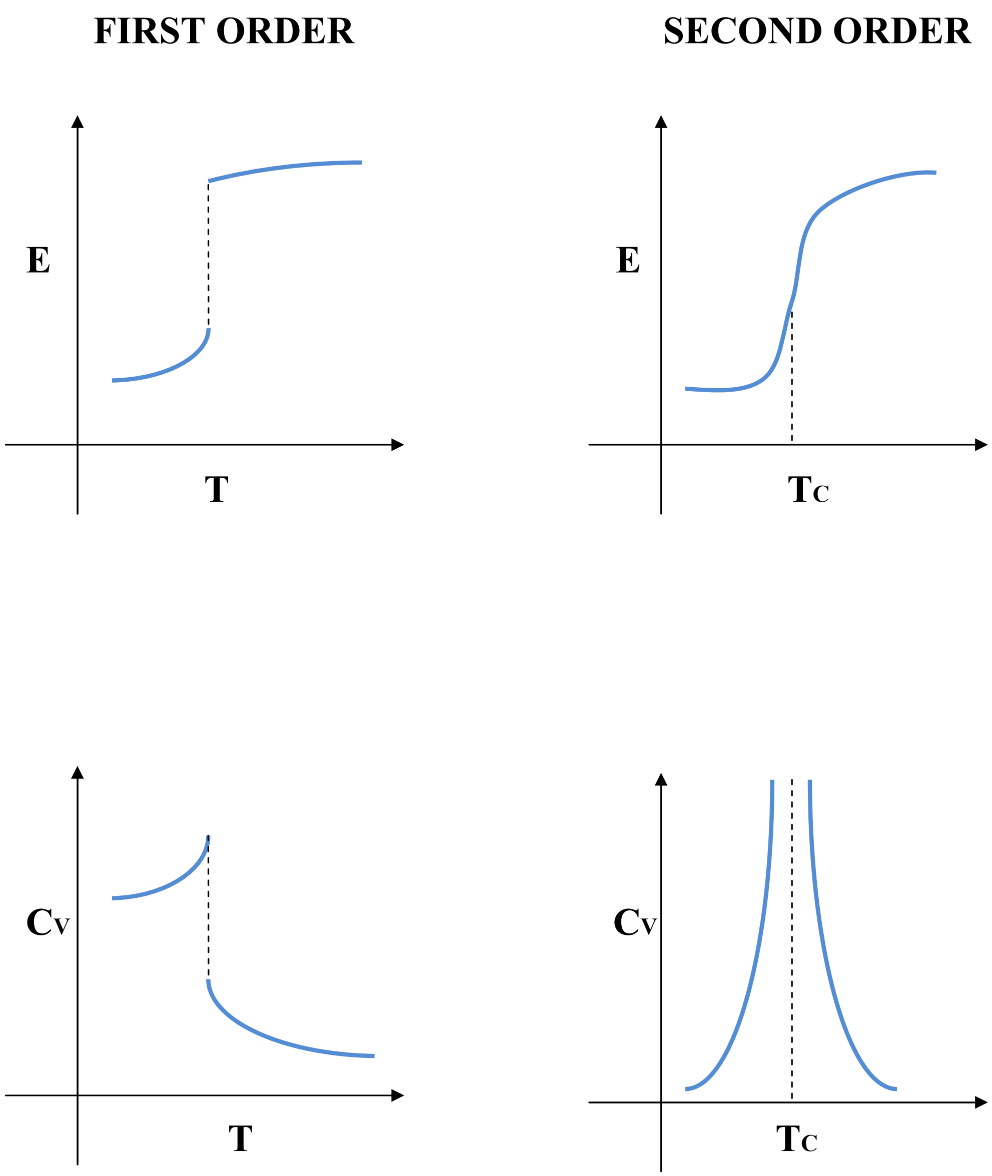

- Discontinuous ϵ – Nonzero Latent Heat– & finite C_v $\rightarrow$ First order PT.
- Continuous ϵ, & diverging C_v $\rightarrow$ Second order PT.
- In(Finite) Correleation Length at 2nd (1st) Order transition.
- "Cross-over" – mere rapid change in ϵ, with maybe a sharp peaked C_v.

Quantum Chromo Dynamics (QCD)

- (Gauge) Theory of interactions of quarks-gluons.
- Similar to structure in theory of electrons & photons (QED).

Quantum Chromo Dynamics (QCD)

- (Gauge) Theory of interactions of quarks-gluons.
- Similar to structure in theory of electrons & photons (QED).
- Many more "photons" (Eight) which carry colour charge & hence interact amongst themselves.
- *Unlike QED*, the coupling is usually very large.

Quantum Chromo Dynamics (QCD)

- (Gauge) Theory of interactions of quarks-gluons.
- Similar to structure in theory of electrons & photons (QED).
- Many more "photons" (Eight) which carry colour charge & hence interact amongst themselves.
- *Unlike QED*, the coupling is usually very large.
- Much richer structure : Quark Confinement, Dynamical Symmetry Breaking..
- Very high interaction (binding) energies. E.g., $M_{Proton} \gg (2m_u + m_d)$, by a factor of 100 $\rightarrow$ Understanding it is knowing where the Visible mass of Universe comes from.

Chiral Symmetry & Effective quark mass

- Spin $1/2$ particle of mass $m \Rightarrow S_z = \pm 1/2$. Let z-axis be along its momentum $\vec{P}$

Chiral Symmetry & Effective quark mass

- Spin 1/2 particle of mass $m \Rightarrow S_z = \pm 1/2$. Let z-axis be along its momentum $\vec{P}$: A) $[S_z \rightarrow]$ along the momentum $[\vec{P} \Longrightarrow]$

  OR

  B) Opposite to it, *i. e.*, $[S_z \leftarrow]$ along $[\vec{P} \Longrightarrow] \quad \equiv \quad [S_z \rightarrow]$ along $[\vec{P} \Longleftarrow]$.

Chiral Symmetry & Effective quark mass

- Spin 1/2 particle of mass $m \Rightarrow S_z = \pm 1/2$. Let z-axis be along its momentum $\vec{P}$: A) $[S_z \rightarrow]$ along the momentum $[\vec{P} \Longrightarrow]$

  OR

  B) Opposite to it, *i. e.*, $[S_z \leftarrow]$ along $[\vec{P} \Longrightarrow] \quad \equiv \quad [S_z \rightarrow]$ along $[\vec{P} \Longleftarrow]$.

- Particle in state A can be transformed to state B by a Lorentz transformation along z-axis.

- The particle must come to rest in between : $m \neq 0$.

Chiral Symmetry & Effective quark mass

- Spin 1/2 particle of mass $m \Rightarrow S_z = \pm 1/2$. Let z-axis be along its momentum $\vec{P}$: A) $[S_z \rightarrow]$ along the momentum $[\vec{P} \Longrightarrow]$

  OR

  B) Opposite to it, *i. e.*, $[S_z \leftarrow]$ along $[\vec{P} \Longrightarrow] \quad \equiv \quad [S_z \rightarrow]$ along $[\vec{P} \Longleftarrow]$.

- Particle in state A can be transformed to state B by a Lorentz transformation along z-axis.

- The particle must come to rest in between : $m \neq 0$.

- For (N_f) massless particles, A or B do **not** change into each other: Chiral Symmetry $(SU(N_f) \times SU(N_f))$.

- Interactions can break the chiral symmetry dynamically, leading to effective masses for these particles.
- Light pions and heavy baryons (protons/neutrons) arise this way in QCD (Y. Nambu, Physics Nobel Prize 2008).

- Interactions can break the chiral symmetry dynamically, leading to effective masses for these particles.

- Light pions and heavy baryons (protons/neutrons) arise this way in QCD (Y. Nambu, Physics Nobel Prize 2008).

- Chiral symmetry **may** get restored at sufficiently high temperatures or densities. Effective mass then 'melts' away, just as magnet loses its magnetic properties on heating.

- New States at High Temperatures/Density expected on basis of models.

- Interactions can break the chiral symmetry dynamically, leading to effective masses for these particles.

- Light pions and heavy baryons (protons/neutrons) arise this way in QCD (Y. Nambu, Physics Nobel Prize 2008).

- Chiral symmetry **may** get restored at sufficiently high temperatures or densities. Effective mass then 'melts' away, just as magnet loses its magnetic properties on heating.

- New States at High Temperatures/Density expected on basis of models.

- Quark-Gluon Plasma is such a phase. It presumably filled our Universe a few microseconds after the Big Bang & can be produced in Relativistic Heavy Ion Collisions.

- Much richer structure in QCD : Quark Confinement, Dynamical Symmetry Breaking.. Lattice QCD should shed light on this all.

QCD Phase diagram

♠ A fundamental aspect – Critical Point in T-μ_B plane;

QCD Phase diagram

♠ A fundamental aspect – Critical Point in T-μ_B plane; Based on symmetries and models, expected QCD Phase Diagram

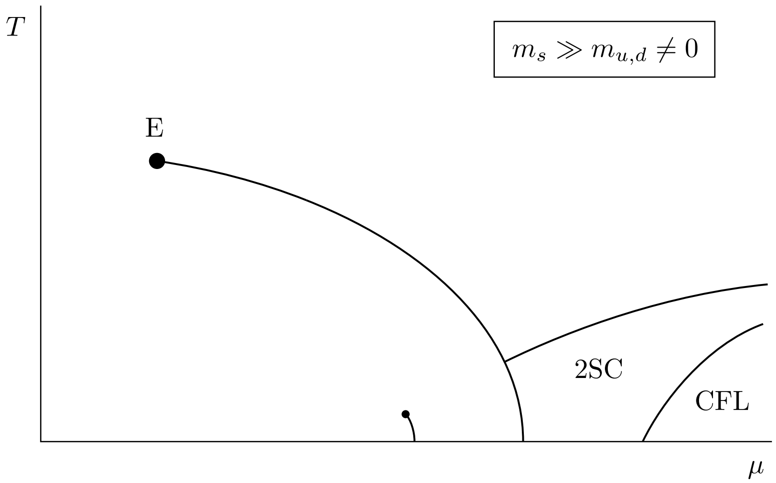

From Rajagopal-Wilczek Review

QCD Phase diagram

♠ A fundamental aspect – Critical Point in T-μ_B plane; Based on symmetries and models, expected QCD Phase Diagram ... but could, however, be ...

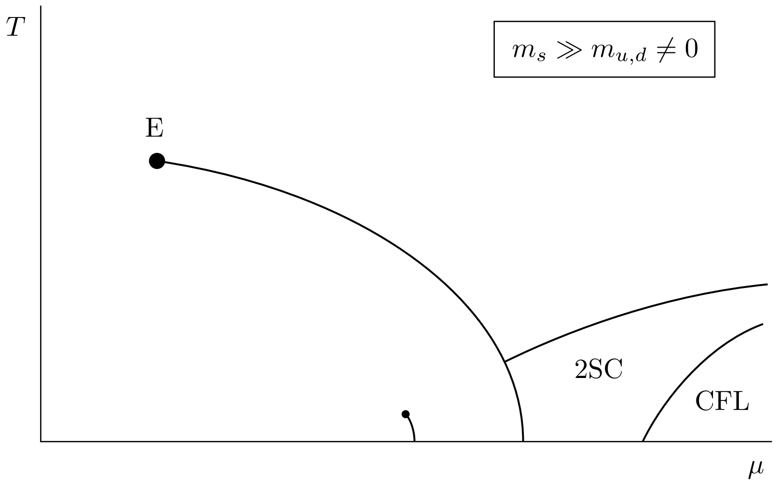

From Rajagopal-Wilczek Review

QCD Phase diagram

♠ A fundamental aspect – Critical Point in T-μ_B plane; Based on symmetries and models, expected QCD Phase Diagram ... but could, however, be ...

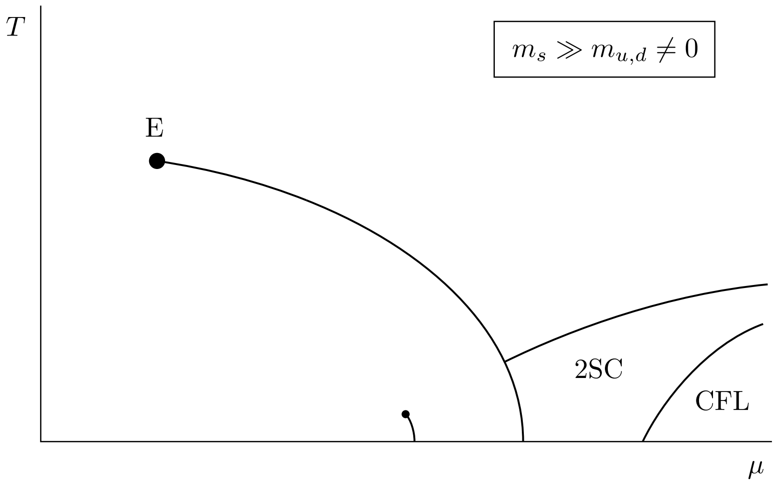

From Rajagopal-Wilczek Review

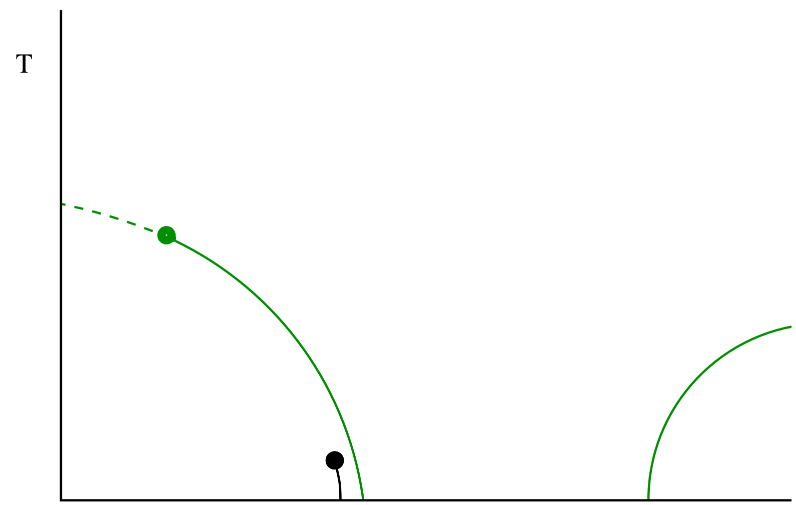

QCD Phase diagram

♠ A fundamental aspect – Critical Point in T-μ_B plane; Based on symmetries and models, expected QCD Phase Diagram ... but could, however, be ... (McLerran-Pisarski 2007; Castorina-RVG-Satz 2010)

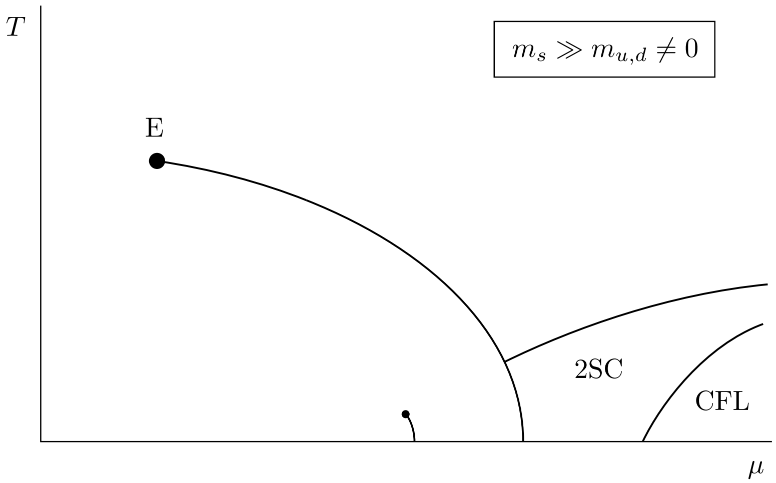

From Rajagopal-Wilczek Review

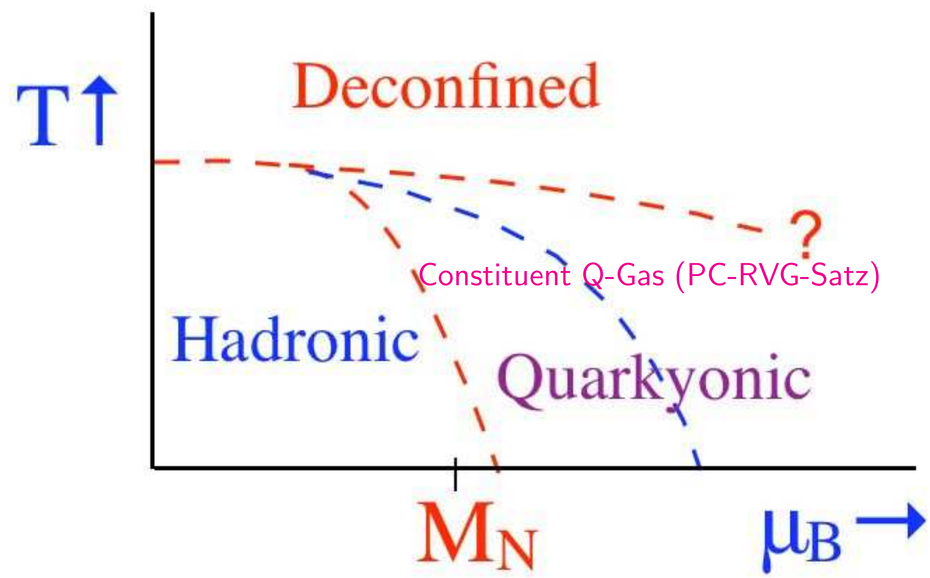

Basic Lattice QCD

- Discrete space-time : Lattice spacing a UV Cut-off.
- Quark fields $\psi(x)$, $\bar{\psi}(x)$ on lattice sites.
- Gluon Fields on links : $U_\mu(x)$

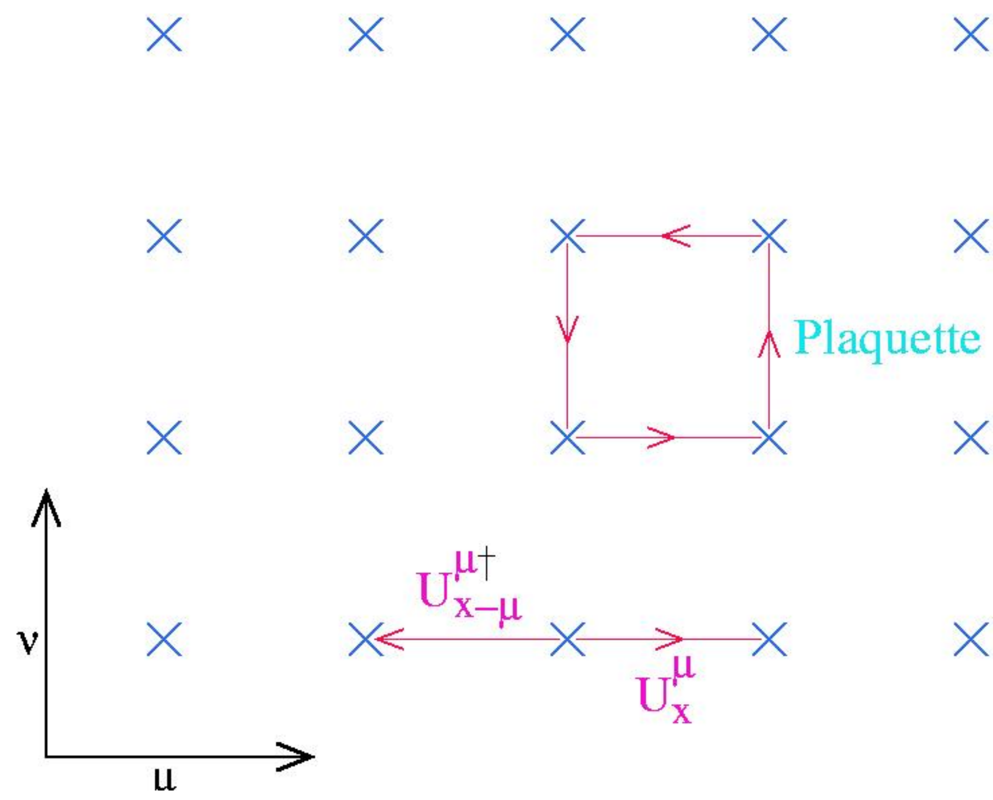

Basic Lattice QCD

- Discrete space-time : Lattice spacing a UV Cut-off.
- Quark fields $\psi(x)$, $\bar{\psi}(x)$ on lattice sites.
- Gluon Fields on links : $U_\mu(x)$
- Gauge invariance : Actions from Closed Wilson loops, e.g., plaquette.
- Fermion Actions : Staggered, Wilson, Overlap, Domain Wall..

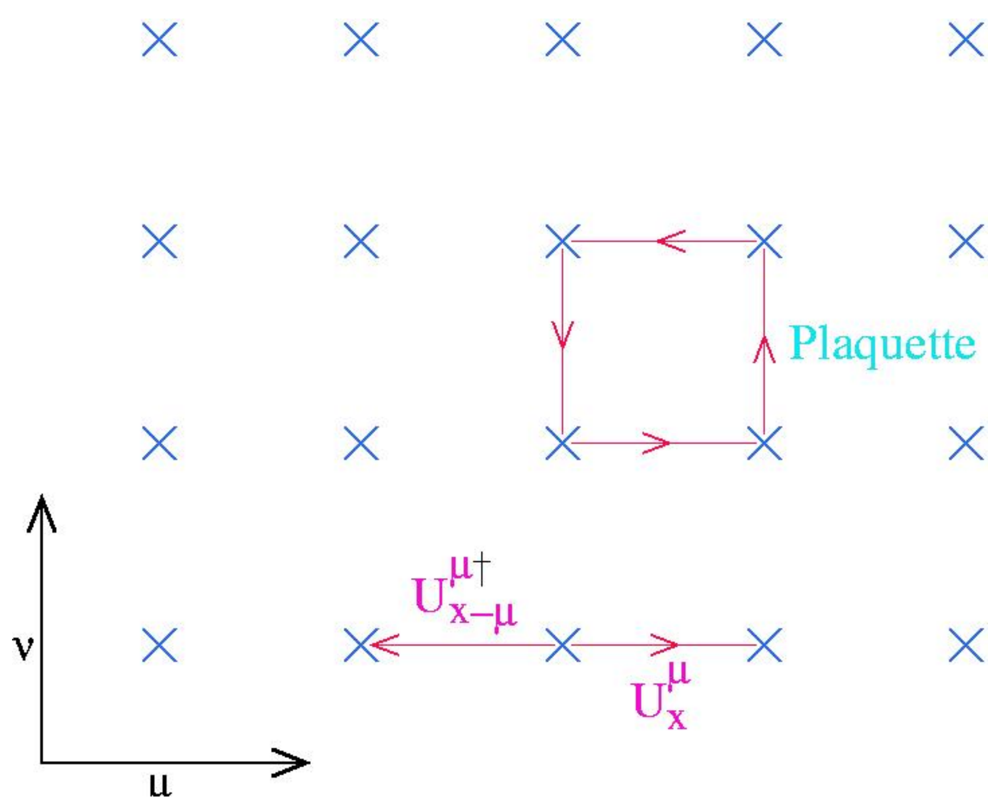

The $\mu \neq 0$ problem

Assuming N_f flavours of quarks, and denoting by μ_f the corresponding chemical potentials, the QCD partition function is

$$\mathcal{Z} = \int DU \exp(-S_G) \ \prod_f \mathrm{Det} \ M(m_f, \mu_f) \quad ,$$

and the thermal expectation value of an observable $\mathcal{O}$ is

$$\langle \mathcal{O} \rangle = \frac{\int DU \exp(-S_G) \ \mathcal{O} \prod_f \mathrm{Det} \ M(m_f, \mu_f)}{\mathcal{Z}} .$$

The $\mu \neq 0$ problem

Assuming N_f flavours of quarks, and denoting by μ_f the corresponding chemical potentials, the QCD partition function is

$$\mathcal{Z} = \int DU \exp(-S_G) \ \prod_f \mathrm{Det} \ \ M(m_f, \mu_f) \quad ,$$

and the thermal expectation value of an observable $\mathcal{O}$ is

$$\langle \mathcal{O} \rangle = \frac{\int DU \exp(-S_G) \ \ \mathcal{O} \prod_f \mathrm{Det} \ \ M(m_f, \mu_f)}{\mathcal{Z}} .$$

Simulations can be done IF Det $M > 0$ for any set of $\{U\}$ as probabilisitc methods are used to evaluate $\langle \mathcal{O} \rangle$.

However, det M is a complex number for any $\mu \neq 0$: The Phase/sign problem

Lattice Approaches

Several Approaches proposed in the past two decades : None as satisfactory as the usual $T \neq 0$ simulations. Still scope for a good/great idea !

Lattice Approaches

Several Approaches proposed in the past two decades : None as satisfactory as the usual $T \neq 0$ simulations. Still scope for a good/great idea !

- Two parameter Re-weighting (Z. Fodor & S. Katz, JHEP 0203 (2002) 014).
- Imaginary Chemical Potential (Ph. de Frocrand & O. Philipsen, NP B642 (2002) 290; M.-P. Lombardo & M. D'Elia PR D67 (2003) 014505).
- Taylor Expansion (R.V. Gavai and S. Gupta, PR D68 (2003) 034506 ; C. Allton et al., PR D68 (2003) 014507).
- Canonical Ensemble (K. -F. Liu, IJMP B16 (2002) 2017, S. Kratochvila and P. de Forcrand, Pos LAT2005 (2006) 167.)
- Complex Langevin (G. Aarts and I. O. Stamatescu, arXiv:0809.5227 and its references for earlier work).

Why Taylor series expansion?

- Ease of taking continuum and thermodynamic limit.

- E.g., exp[ΔS] factor makes this exponentially tough for re-weighting.

Why Taylor series expansion?

- Ease of taking continuum and thermodynamic limit.
- E.g., exp$[\Delta S]$ factor makes this exponentially tough for re-weighting.
- Discretization errors propagate in an unknown manner in re-weighting.
- Better control of systematic errors.

Why Taylor series expansion?

- Ease of taking continuum and thermodynamic limit.
- E.g., $\exp[\Delta S]$ factor makes this exponentially tough for re-weighting.
- Discretization errors propagate in an unknown manner in re-weighting.
- Better control of systematic errors.

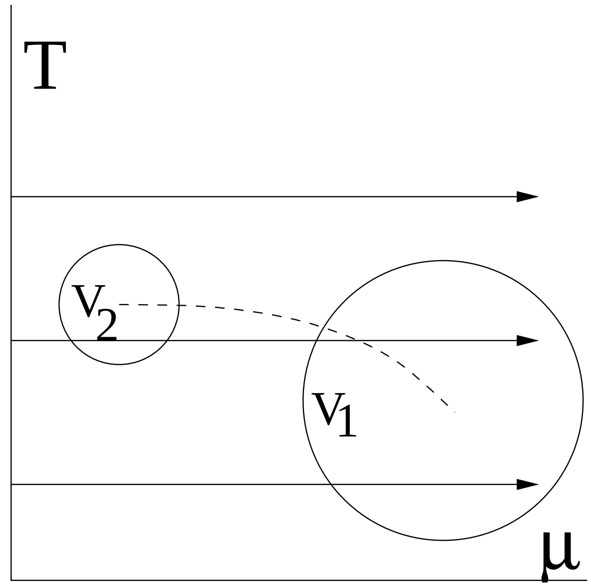

We study volume dependence at several T to i) bracket the critical region and then to ii) track its change as a function of volume.

How Do We Do This Expansion?

Canonical definitions yield various number densities and susceptibilities :

$$n_i = \frac{T}{V}\frac{\partial \ln \mathcal{Z}}{\partial \mu_i} \text{ and } \qquad \chi_{ij} = \frac{T}{V}\frac{\partial^2 \ln \mathcal{Z}}{\partial \mu_i \partial \mu_j} \quad .$$

These are also useful by themselves both theoretically and for Heavy Ion Physics (Flavour correlations, $\lambda_s \ldots$)

Denoting higher order susceptibilities by χ_{n_u,n_d}, the pressure P has the expansion in μ:

$$\frac{\Delta P}{T^4} \equiv \frac{P(\mu,T)}{T^4} - \frac{P(0,T)}{T^4} = \sum_{n_u,n_d} \chi_{n_u,n_d} \frac{1}{n_u!}\left(\frac{\mu_u}{T}\right)^{n_u} \frac{1}{n_d!}\left(\frac{\mu_d}{T}\right)^{n_d} \tag{1}$$

How Do We Do This Expansion?

Canonical definitions yield various number densities and susceptibilities :

$$n_i = \frac{T}{V}\frac{\partial \ln \mathcal{Z}}{\partial \mu_i} \text{ and } \qquad \chi_{ij} = \frac{T}{V}\frac{\partial^2 \ln \mathcal{Z}}{\partial \mu_i \partial \mu_j} \quad .$$

These are also useful by themselves both theoretically and for Heavy Ion Physics (Flavour correlations, $\lambda_s \ldots$)

Denoting higher order susceptibilities by χ_{n_u,n_d}, the pressure P has the expansion in μ:

$$\frac{\Delta P}{T^4} \equiv \frac{P(\mu,T)}{T^4} - \frac{P(0,T)}{T^4} = \sum_{n_u,n_d} \chi_{n_u,n_d} \frac{1}{n_u!}\left(\frac{\mu_u}{T}\right)^{n_u} \frac{1}{n_d!}\left(\frac{\mu_d}{T}\right)^{n_d} \tag{1}$$

- From this expansion, a series for baryonic susceptibility can be constructed. Its radius of convergence gives the nearest critical point.

- Successive estimates for the radius of convergence can be obtained from these using $\sqrt{\frac{n(n+1)\chi_B^{(n+1)}}{\chi_B^{(n+3)}}}$ or $\left(n!\frac{\chi_B^{(2)}}{\chi_B^{(n+2)}}\right)^{1/n}$. We use both definitions and look for consistency.

- All coefficients of the series must be POSITIVE for the critical point to be at real μ, and thus physical.

- We (Gavai-Gupta '05, '09) use up to 8^{th} order. B-RBC so far has up to 6^{th} order.

- 10th & even 12th order may be possible : Ideas to extend to higher orders are emerging (Gavai-Sharma PRD 2012 & PRD 2010) which save up to 60 % computer time.

- From this expansion, a series for baryonic susceptibility can be constructed. Its radius of convergence gives the nearest critical point.

- Successive estimates for the radius of convergence can be obtained from these using $\sqrt{\frac{n(n+1)\chi_B^{(n+1)}}{\chi_B^{(n+3)}}}$ or $\left(n!\frac{\chi_B^{(2)}}{\chi_B^{(n+2)}}\right)^{1/n}$. We use both definitions and look for consistency.

- All coefficients of the series must be POSITIVE for the critical point to be at real μ, and thus physical.

- We (Gavai-Gupta '05, '09) use up to 8^{th} order. B-RBC so far has up to 6^{th} order.

- 10th & even 12th order may be possible : Ideas to extend to higher orders are emerging (Gavai-Sharma PRD 2012 & PRD 2010) which save up to 60 % computer time.

- From this expansion, a series for baryonic susceptibility can be constructed. Its radius of convergence gives the nearest critical point.

- Successive estimates for the radius of convergence can be obtained from these using $\sqrt{\frac{n(n+1)\chi_B^{(n+1)}}{\chi_B^{(n+3)}}}$ or $\left(n!\frac{\chi_B^{(2)}}{\chi_B^{(n+2)}}\right)^{1/n}$. We use both definitions and look for consistency.

- All coefficients of the series must be POSITIVE for the critical point to be at real μ, and thus physical.

- We (Gavai-Gupta '05, '09) use up to 8^{th} order. B-RBC so far has up to 6^{th} order.

- 10th & even 12th order may be possible : Ideas to extend to higher orders are emerging (Gavai-Sharma PRD 2012 & PRD 2010) which save up to 60 % computer time.

The Susceptibilities

All susceptibilities can be written as traces of products of M^{-1} and various derivatives of M.

At leading order,

$$\chi_{20} = \left(\frac{T}{V}\right)[\langle \mathcal{O}_2 + \mathcal{O}_{11} \rangle], \qquad \chi_{11} = \left(\frac{T}{V}\right)[\langle \mathcal{O}_{11} \rangle]$$

Here $\mathcal{O}_2 = \mathrm{Tr}\ M^{-1}M'' - \mathrm{Tr}\ M^{-1}M'M^{-1}M'$, and $\mathcal{O}_{11} = (\mathrm{Tr}\ M^{-1}M')^2$, and the traces are estimated by a stochastic method (Gottlieb et al., PRL '87):

$\mathrm{Tr}\ A = \sum_{i=1}^{N_v} R_i^\dagger A R_i / 2N_v$, and $(\mathrm{Tr}\ A)^2 = 2\sum_{i>j=1}^{L} (\mathrm{Tr}\ A)_i (\mathrm{Tr}\ A)_j / L(L-1)$, where R_i is a complex vector from a set of N_v subdivided in L independent sets.

The Susceptibilities

All susceptibilities can be written as traces of products of M^{-1} and various derivatives of M.

At leading order,

$$\chi_{20} = \left(\frac{T}{V}\right)[\langle \mathcal{O}_2 + \mathcal{O}_{11}\rangle], \qquad \chi_{11} = \left(\frac{T}{V}\right)[\langle \mathcal{O}_{11}\rangle]$$

Here $\mathcal{O}_2 = \mathrm{Tr}\ M^{-1}M'' - \mathrm{Tr}\ M^{-1}M'M^{-1}M'$, and $\mathcal{O}_{11} = (\mathrm{Tr}\ M^{-1}M')^2$, and the traces are estimated by a stochastic method (Gottlieb et al., PRL '87):

$\mathrm{Tr}\ A = \sum_{i=1}^{N_v} R_i^\dagger A R_i / 2N_v$, and $(\mathrm{Tr}\ A)^2 = 2\sum_{i>j=1}^{L} (\mathrm{Tr}\ A)_i (\mathrm{Tr}\ A)_j / L(L-1)$, where R_i is a complex vector from a set of N_v subdivided in L independent sets.

Higher order NLS are more involved. E.g.,

$$\chi_{40} = \frac{T}{V}\left[\left\langle \mathcal{O}_{1111} + 6\mathcal{O}_{112} + 4\mathcal{O}_{13} + 3\mathcal{O}_{22} + \mathcal{O}_4 \right\rangle - 3\left\langle \mathcal{O}_{11} + \mathcal{O}_2 \right\rangle^2\right].$$

Here the notation $\mathcal{O}_{ij\dots l}$ stands for the product, $\mathcal{O}_i\mathcal{O}_j \cdots O_l$ and
$\mathcal{O}_3 = 2\ \mathrm{Tr}\ (M^{-1}M')^3 - 3\ \mathrm{Tr}\ M^{-1}M'M^{-1}M'' + \mathrm{Tr}\ M^{-1}M'''$,
$\mathcal{O}_4 = -6\ \mathrm{Tr}\ (M^{-1}M')^4 + 12\ \mathrm{Tr}\ (M^{-1}M')^2M^{-1}M'' - 3\ \mathrm{Tr}\ (M^{-1}M'')^2 -$
$3\ \mathrm{Tr}\ M^{-1}M'M^{-1}M''' + \mathrm{Tr}\ M^{-1}M''''$.

At the 8th order, terms involve operators up to $\mathcal{O}_8$ which in turn have terms up to 8 quark propagators and combinations of M' and M''. In fact, the entire evaluation of the χ_{80} needs 20 inversions of Dirac matrix.

This can be reduced to 8 inversions using an action linear in μ (Gavai-Sharma PRD 2012 & PRD 2010), leading still to results in agreement with that exponential in μ.

Higher order NLS are more involved. E.g.,

$$\chi_{40} = \frac{T}{V}\left[\left\langle \mathcal{O}_{1111} + 6\mathcal{O}_{112} + 4\mathcal{O}_{13} + 3\mathcal{O}_{22} + \mathcal{O}_4 \right\rangle - 3\left\langle \mathcal{O}_{11} + \mathcal{O}_2 \right\rangle^2\right].$$

Here the notation $\mathcal{O}_{ij\cdots l}$ stands for the product, $\mathcal{O}_i\mathcal{O}_j \cdots O_l$ and
$\mathcal{O}_3 = 2\ \mathrm{Tr}\ (M^{-1}M')^3 - 3\ \mathrm{Tr}\ M^{-1}M'M^{-1}M'' + \mathrm{Tr}\ M^{-1}M'''$,
$\mathcal{O}_4 = -6\ \mathrm{Tr}\ (M^{-1}M')^4 + 12\ \mathrm{Tr}\ (M^{-1}M')^2M^{-1}M'' - 3\ \mathrm{Tr}\ (M^{-1}M'')^2 -$
$3\ \mathrm{Tr}\ M^{-1}M'M^{-1}M''' + \mathrm{Tr}\ M^{-1}M''''$.

At the 8th order, terms involve operators up to $\mathcal{O}_8$ which in turn have terms up to 8 quark propagators and combinations of M' and M''. In fact, the entire evaluation of the χ_{80} needs 20 inversions of Dirac matrix.

This can be reduced to 8 inversions using an action linear in μ (Gavai-Sharma PRD 2012 & PRD 2010), leading still to results in agreement with that exponential in μ.

Our Simulations & Results

- Staggered fermions with $N_f = 2$ of $m/T_c = 0.1$; R-algorithm used.
- $m_\pi/m_\rho = 0.31 \pm 0.01$ (MILC); Kept the same as $a \to 0$ (on all N_t).
- Earlier Lattice : 4 $\times N_s^3$, $N_s =$ 8, 10, 12, 16, 24 (Gavai-Gupta, PRD 2005)
  Finer Lattice : 6 $\times N_s^3$, $N_s =$ 12, 18, 24 (Gavai-Gupta, PRD 2009).

Our Simulations & Results

- Staggered fermions with $N_f = 2$ of $m/T_c = 0.1$; R-algorithm used.
- $m_\pi/m_\rho = 0.31 \pm 0.01$ (MILC); Kept the same as $a \to 0$ (on all N_t).
- Earlier Lattice : 4 $\times N_s^3$, N_s = 8, 10, 12, 16, 24 (Gavai-Gupta, PRD 2005)
  Finer Lattice : 6 $\times N_s^3$, N_s = 12, 18, 24 (Gavai-Gupta, PRD 2009).
- Even finer Lattice : 8 $\times 32^3$ — This Talk (Datta-RVG-Gupta, arXiv: 1210.6784)
  Aspect ratio, N_s/N_t, maintained four to reduce finite volume effects.
- Simulations made at T/T_c = 0.90, 0.92, 0.94, 0.96, 0.98, 1.00, 1.02, 1.12, 1.5 and 2.01. Typical stat. 100-200 in max autocorrelation units.
- T_c — defined by the peak of Polyakov loop susceptibility.

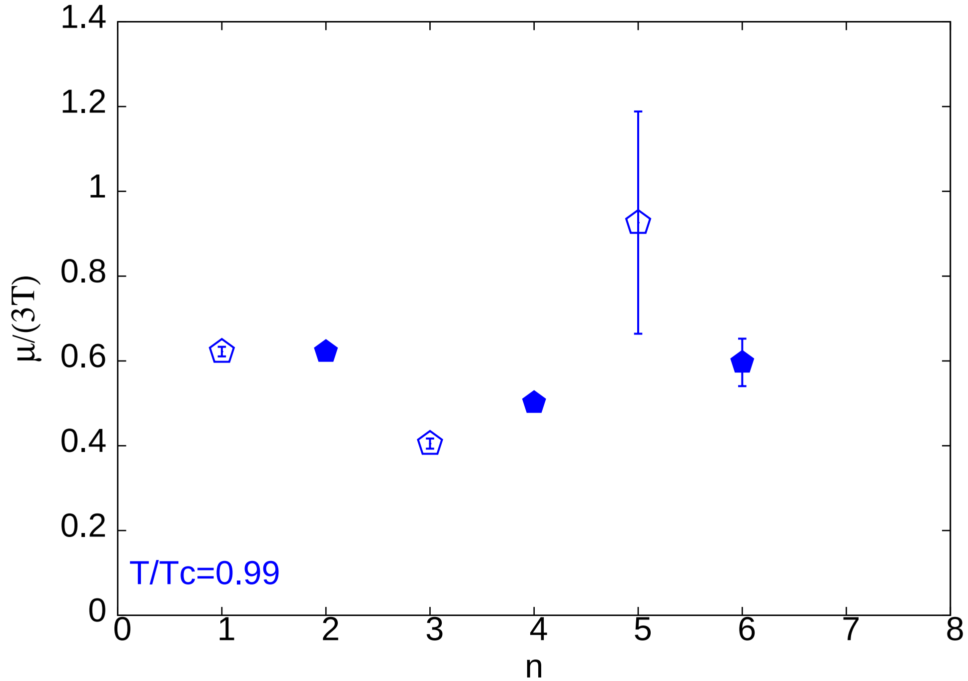
1.4
1.2
1
0.8
0.6
0.4
0.2
0
μ/(3T)
T/Tc=0.99
0
1
2
3
4
5
6
7
8
n

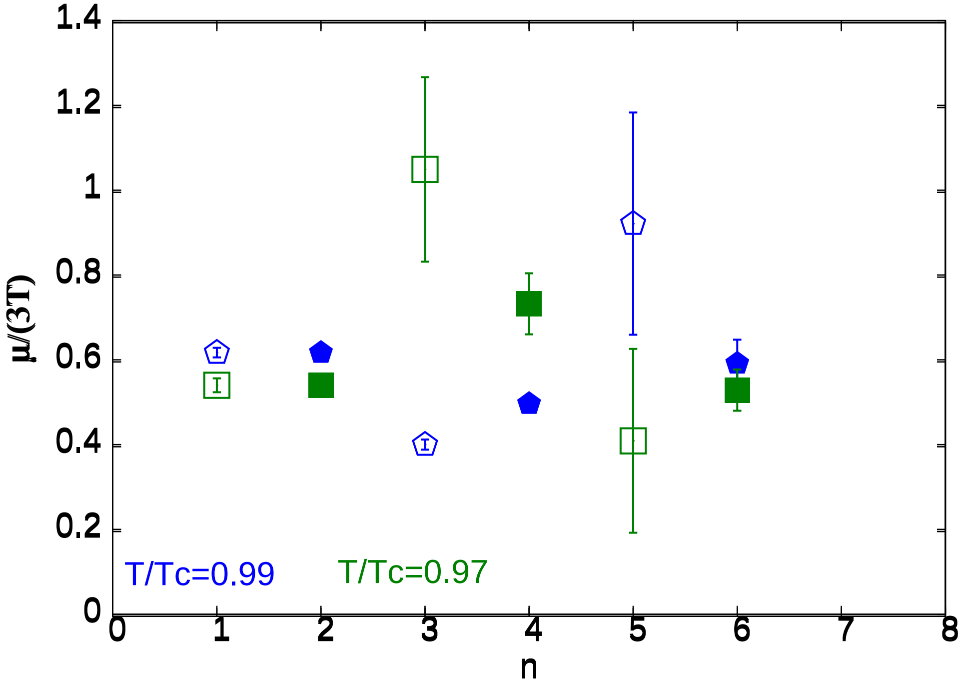

1.4
1.2
1
0.8
0.6
0.4
0.2
0
μ/(3T)
T/Tc=0.99
T/Tc=0.97
0
1
2
3
4
5
6
7
8
n

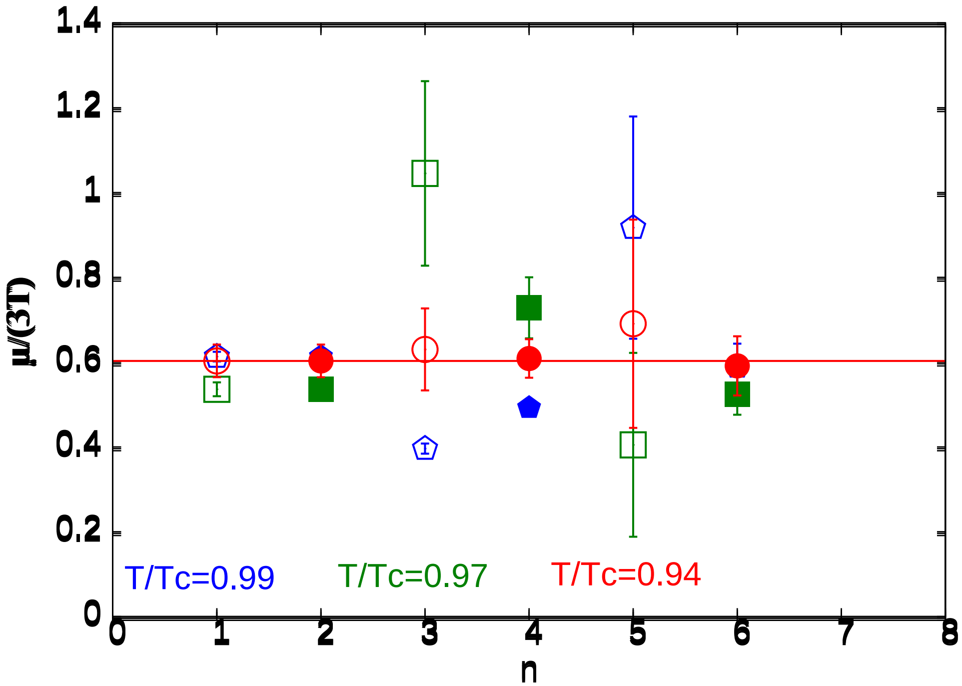

1.4
1.2
1
0.8
0.6
0.4
0.2
0
μ/(3T)
0
1
2
3
4
5
6
7
8
n
T/Tc=0.99
T/Tc=0.97
T/Tc=0.94

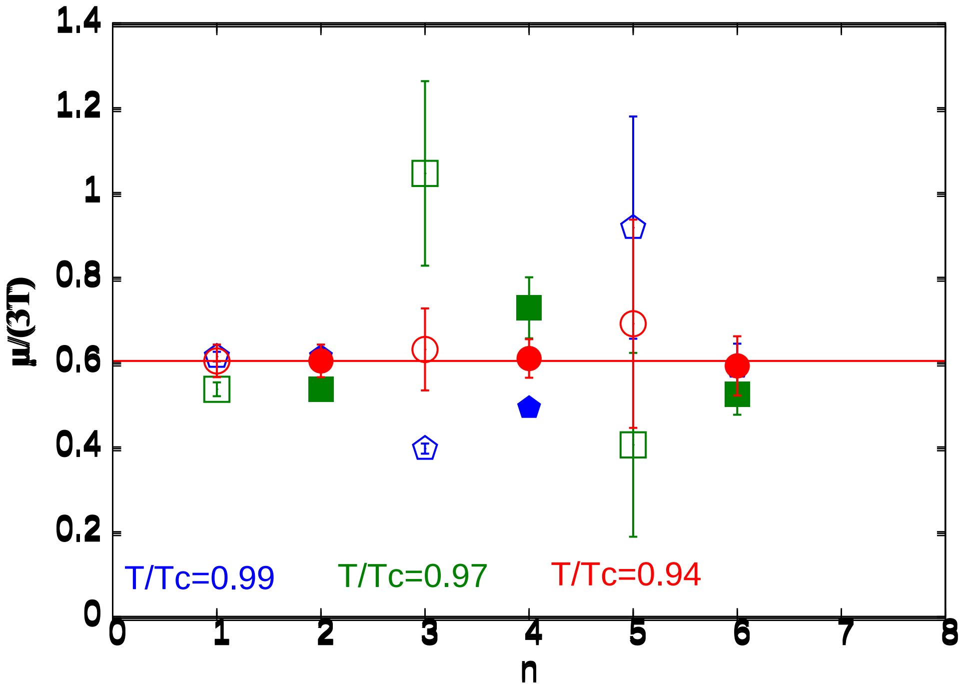

- $\frac{T^E}{T_c} = 0.94 \pm 0.01$, and $\frac{\mu_B^E}{T^E} = 1.8 \pm 0.1$ for finer lattice: Our earlier coarser lattice result was $\mu_B^E/T^E = 1.3 \pm 0.3$. Infinite volume result: $\downarrow$ to 1.1(1)

- Critical point at $\mu_B/T \sim 1 - 2$.

Cross Check on μ^E/T^E

♠ Use Padé approximants for the series to estimate the radius of convergence.

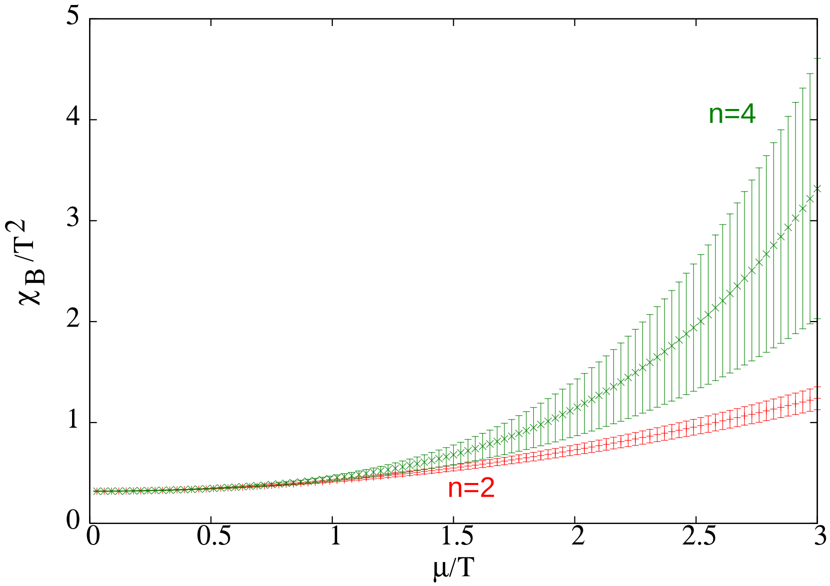

Cross Check on μ^E/T^E

♠ Use Padé approximants for the series to estimate the radius of convergence.

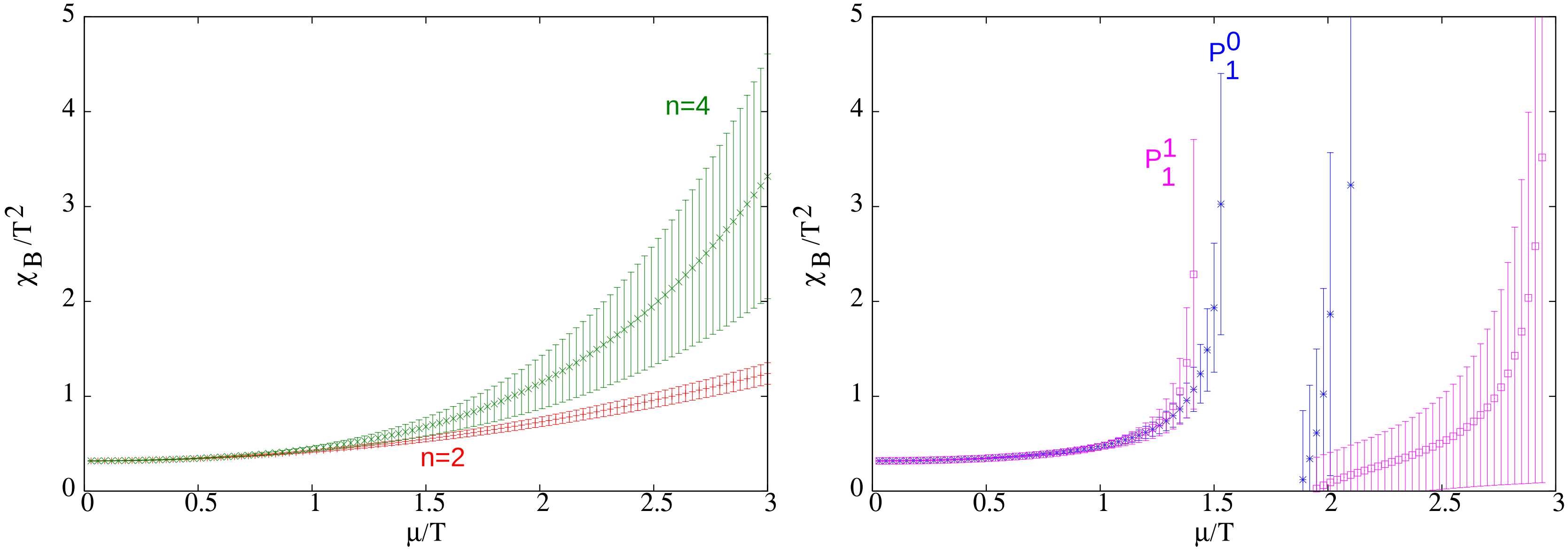

♠ Use Padé approximants for the series to estimate the radius of convergence.

♡ Consistent Window with our other estimates.

χ_2 for $N_t = 8$, 6, and 4 lattices

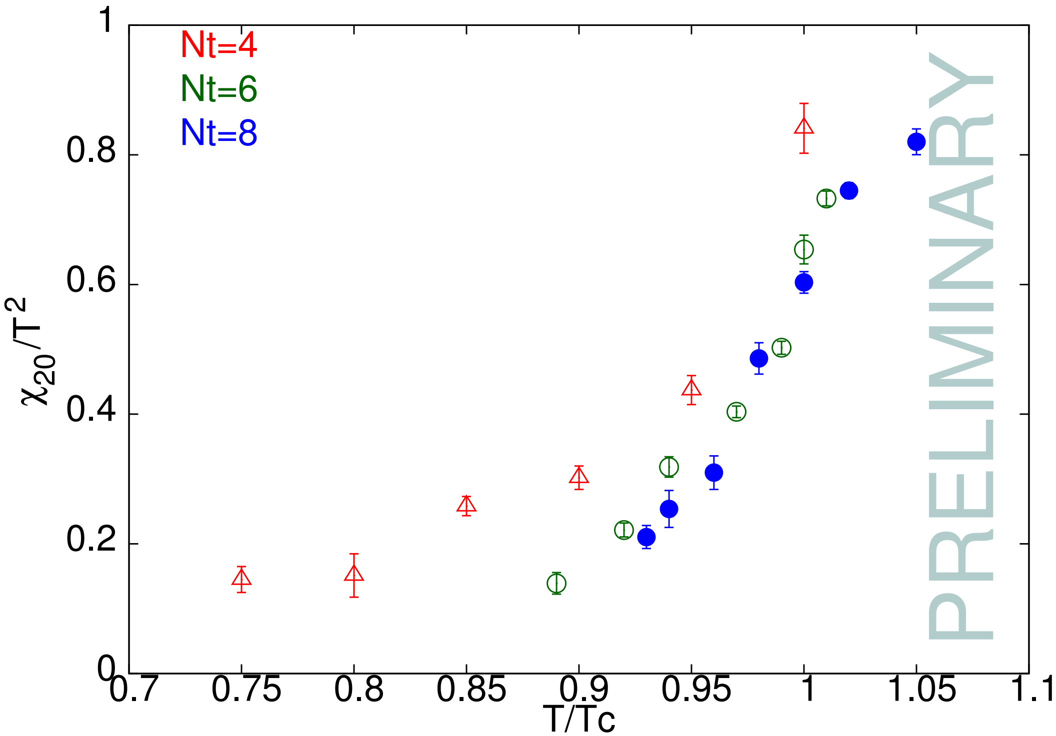

♠ $N_t = 8$ (Datta-Gavai-Gupta, Quark Matter 2012 & arXiv: 1210.6784) and 6 (Gavai-Gupta, PRD '09) results agree.

♡ $\beta_c(N_t = 8)$ agrees with Gottlieb et al. PR D47,1993.

Radius of Convergence result

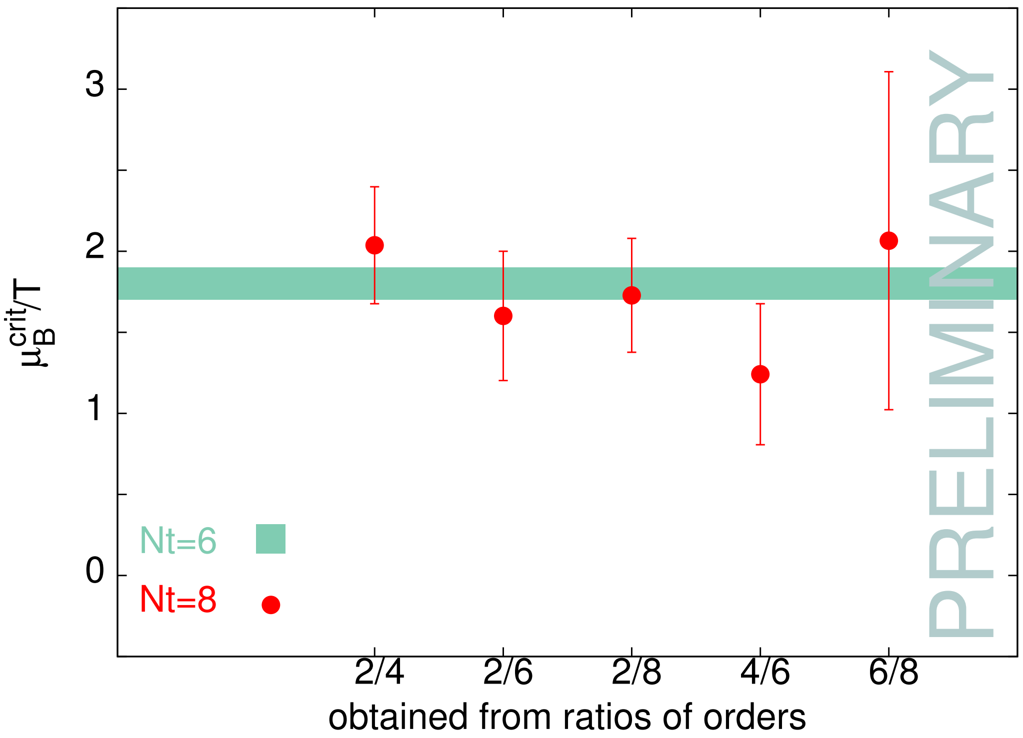

♠ At our (T_E, μ_E) for $N_t = 6$, the ratios display constancy for $N_t = 8$ as well.

♡ Currently : Similar results at neighbouring $T/T_c \Longrightarrow$ a larger ΔT at same μ_B^E.

Critical Point : Inching Towards Continuum

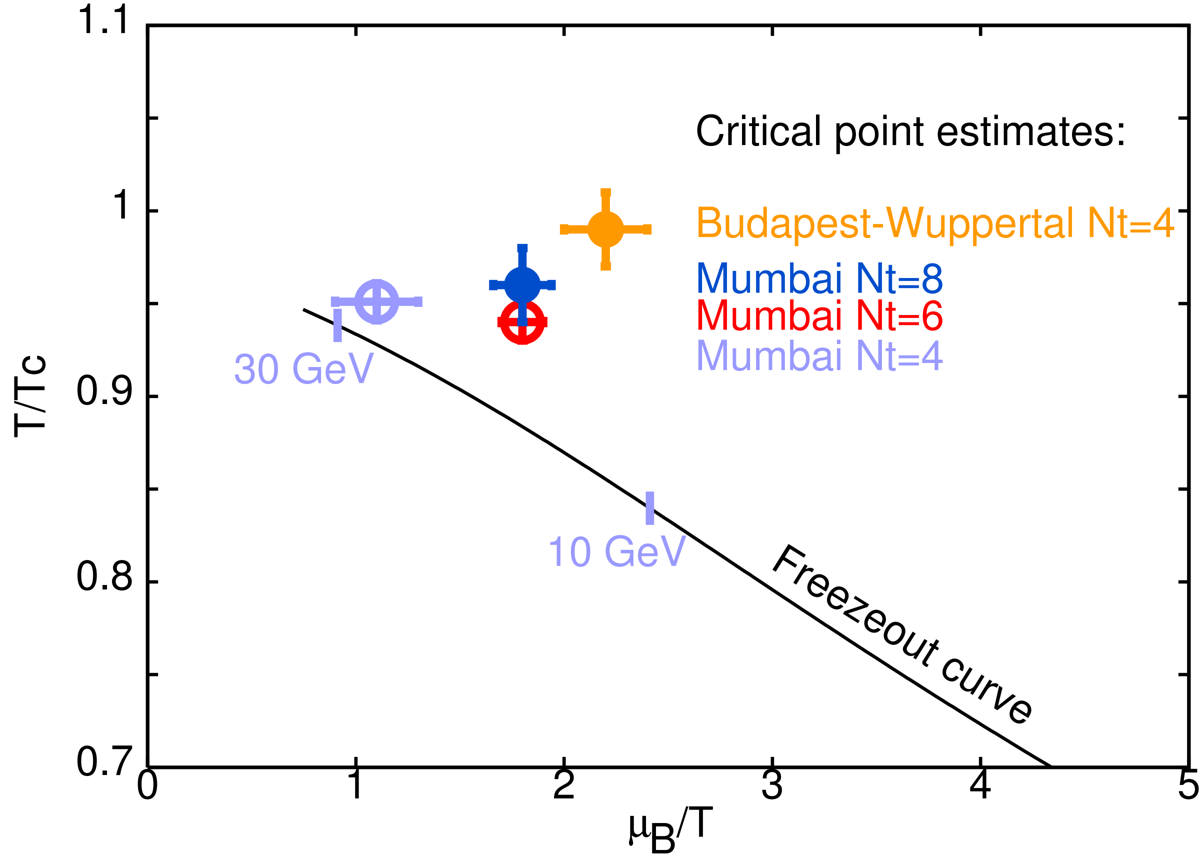

Searching Experimentally

- Exploit the facts i) susceptibilities diverge near the critical point and ii) decreasing $\sqrt{s}$ increases μ_B (Rajagopal, Shuryak & Stephanov PRD 1999)
- Look for nonmontonic dependence of the event-by-event fluctuations with colliding energy.

Searching Experimentally

- Exploit the facts i) susceptibilities diverge near the critical point and ii) decreasing $\sqrt{s}$ increases μ_B (Rajagopal, Shuryak & Stephanov PRD 1999)

- Look for nonmontonic dependence of the event-by-event fluctuations with colliding energy. NA49 results (C. Roland NA49, J.Phys. G30 (2004) S1381-S1384)

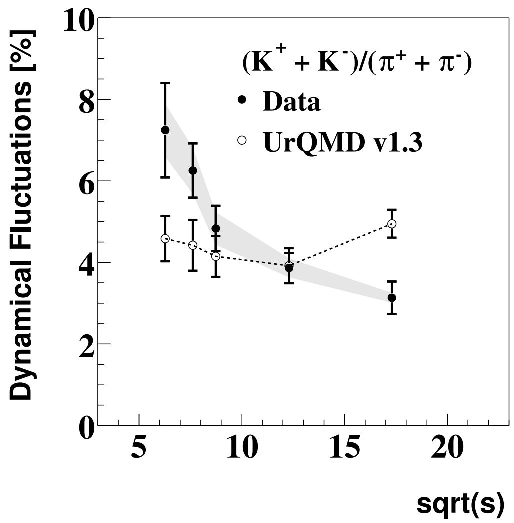

Searching Experimentally

- Exploit the facts i) susceptibilities diverge near the critical point and ii) decreasing $\sqrt{s}$ increases μ_B (Rajagopal, Shuryak & Stephanov PRD 1999)

- Look for nonmontonic dependence of the event-by-event fluctuations with colliding energy. NA49 results (C. Roland NA49, J.Phys. G30 (2004) S1381-S1384)

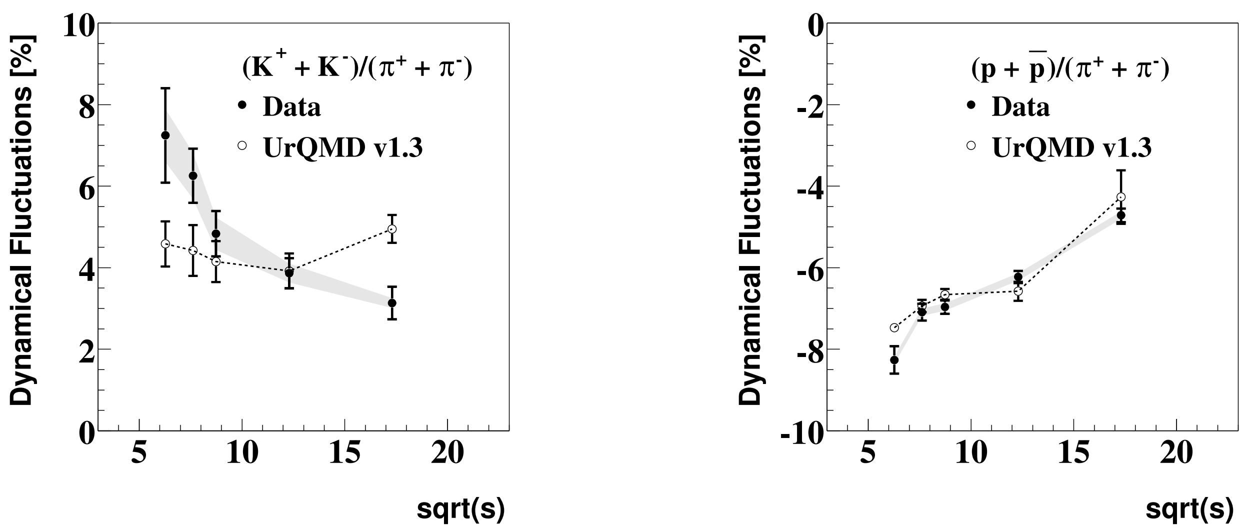

- Fluctuations in mean p_T of low p_T pions.

- Fluctuations in mean p_T of low p_T pions. (K. Grebieszkow, CPOD workshop 2007, GSI, Darmstadt)

Fluctuations due to the critical point should be dominated by fluctuations of pions with $p_T \leq 500$ MeV/c

M. Stephanov, K. Rajagopal, E. V. Shuryak (Phys. Rev. **D60**, 114028, 1999):

suggestion to do analysis with several upper p_T cuts

$p_T < 750$ MeV/c

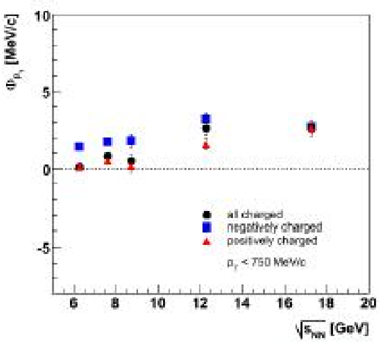

$p_T < 500$ MeV/c

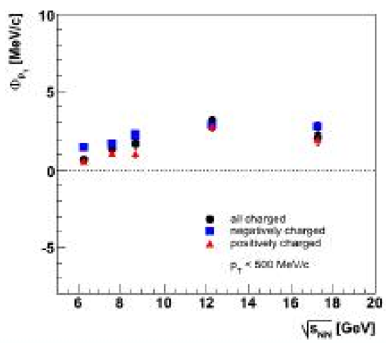

$p_T < 250$ MeV/c

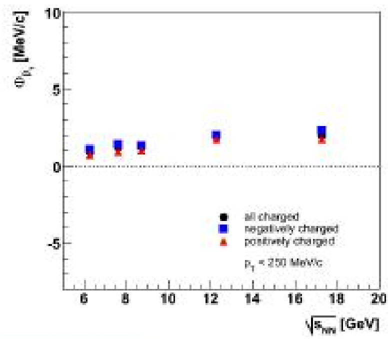

No significant energy dependence of Φ_{PT} measure
also when low transverse momenta are selected.

Remark: predicted fluctuations at the critical point should result in $\Phi_{PT} \cong 20$ MeV/c, the effect of limited acceptance of NA49 reduces them to $\Phi_{PT} \cong$ **10 MeV/c**

Lattice predictions along the freezeout curve

- Hadron yields well described using Statistical Models, leading to a freezeout curve in the T-μ_B plane. (Andronic, Braun-Munzinger & Stachel, PLB 2009 ; Oeschler, Cleymans, Redlich & Wheaton, 2009)

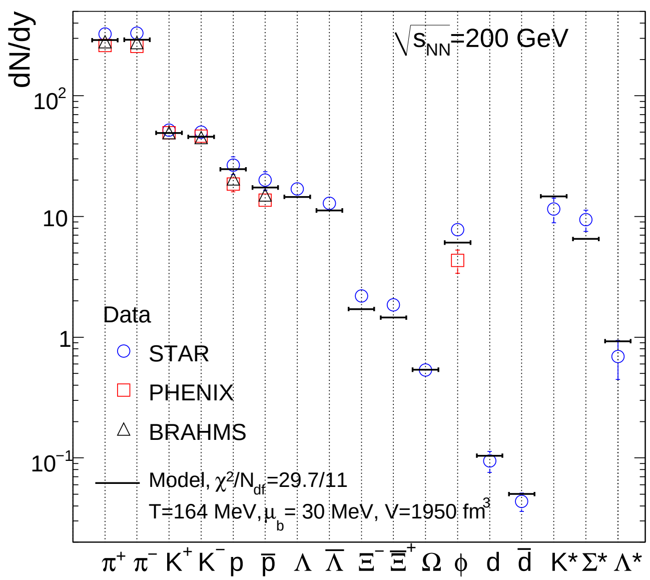

Lattice predictions along the freezeout curve

- Hadron yields well described using Statistical Models, leading to a freezeout curve in the T-μ_B plane. (Andronic, Braun-Munzinger & Stachel, PLB 2009 ; Oeschler, Cleymans, Redlich & Wheaton, 2009)

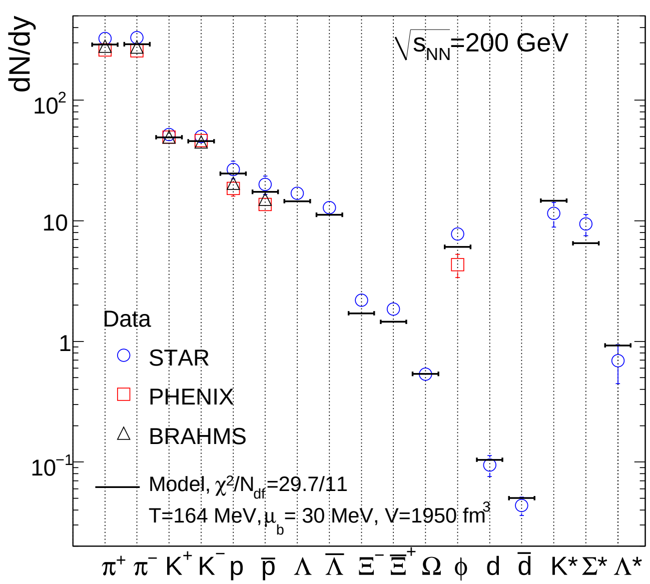

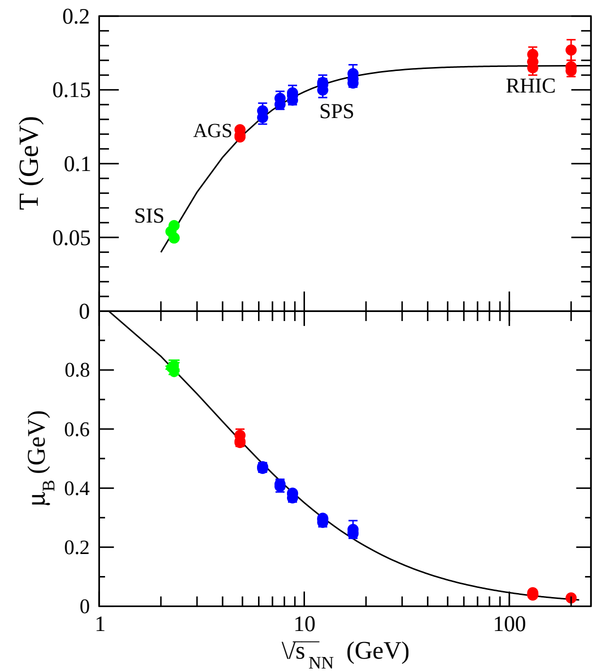

- Plotting these results in the T-μ_B plane, one has the freezeout curve, which was shown to correspond the $\langle E \rangle / \langle N \rangle \simeq 1$. (Cleymans and Redlich, PRL 1998)

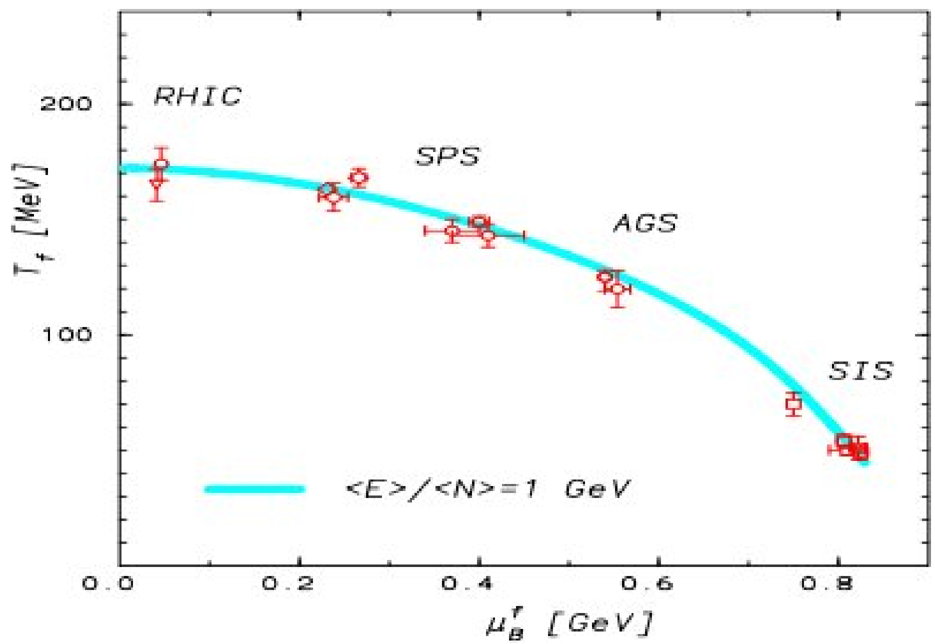

(From Braun-Munzinger, Redlich and Stachel nucl-th/0304013)

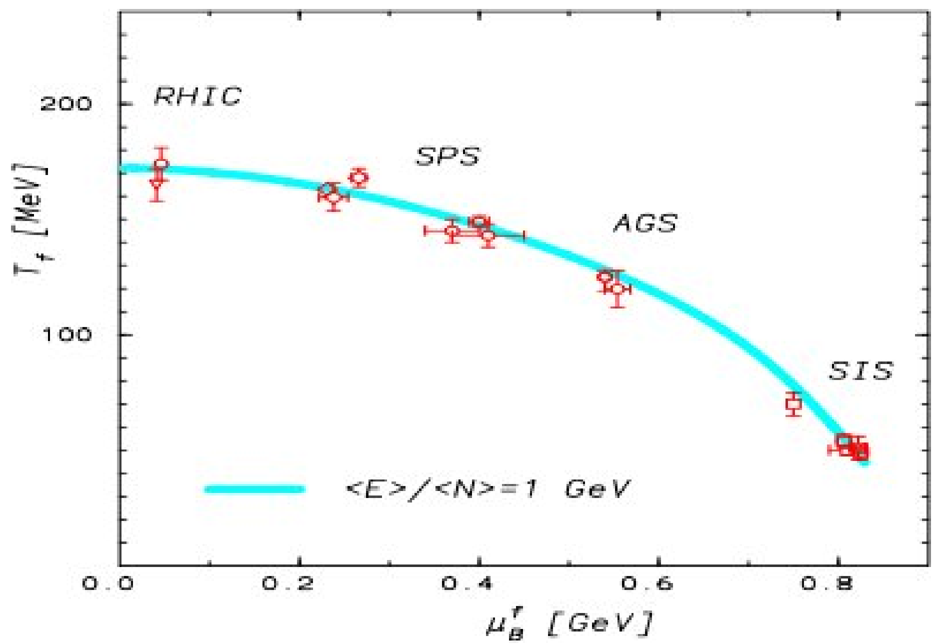

(From Braun-Munzinger, Redlich and Stachel nucl-th/0304013)

- Note : Freeze-out curve is based soled on data on hadron yields, & gives the (T, μ) accessible in heavy-ion experiments.

- Our Key Proposal : Use the freezeout curve from hadron abundances to *predict* fluctuations using lattice QCD along it. (Gavai-Gupta, TIFR/TH/10-01, arXiv 1001.3796)

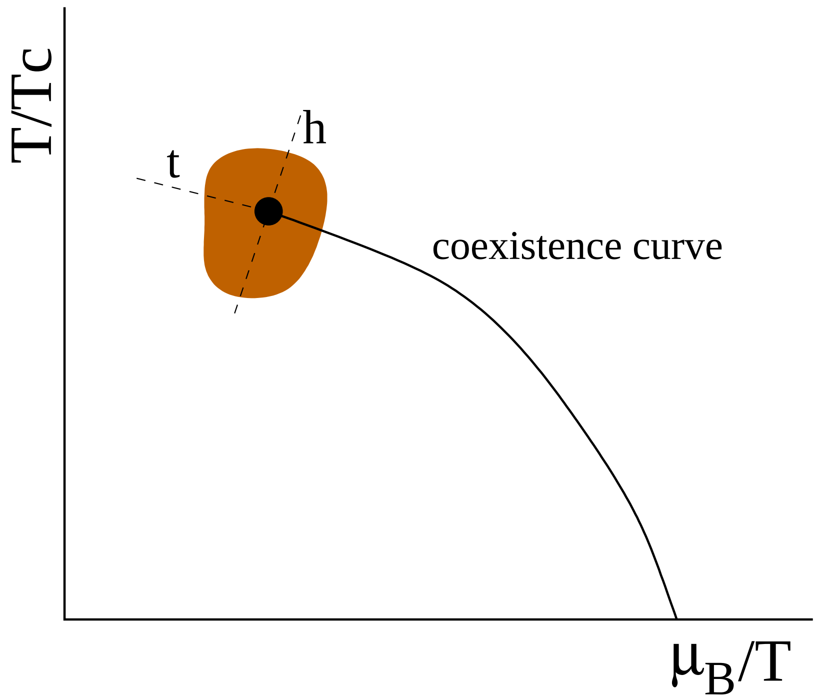

T/Tc
h
t
coexistence curve
μ_B/T

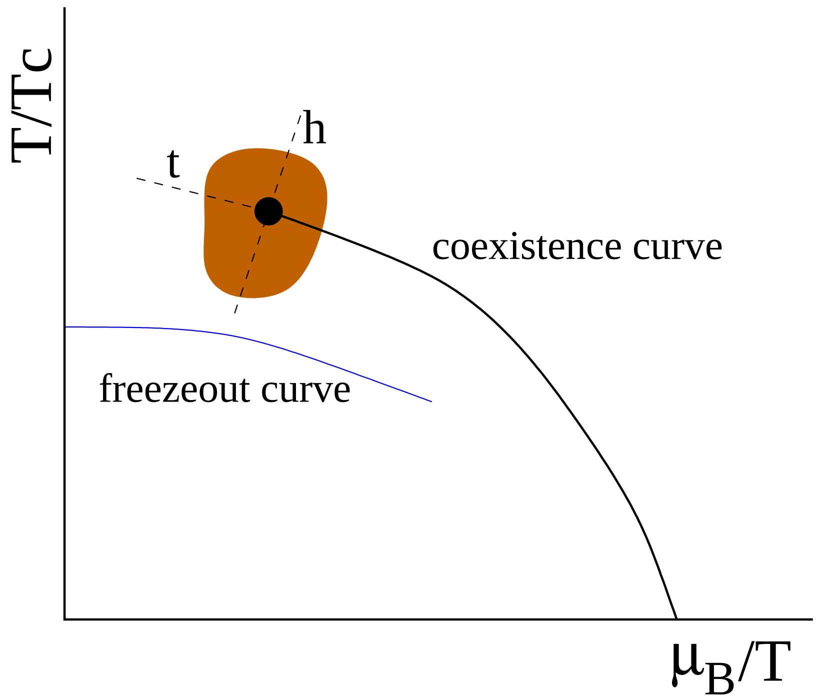
T/Tc
h
t
coexistence curve
freezeout curve
μ_B/T

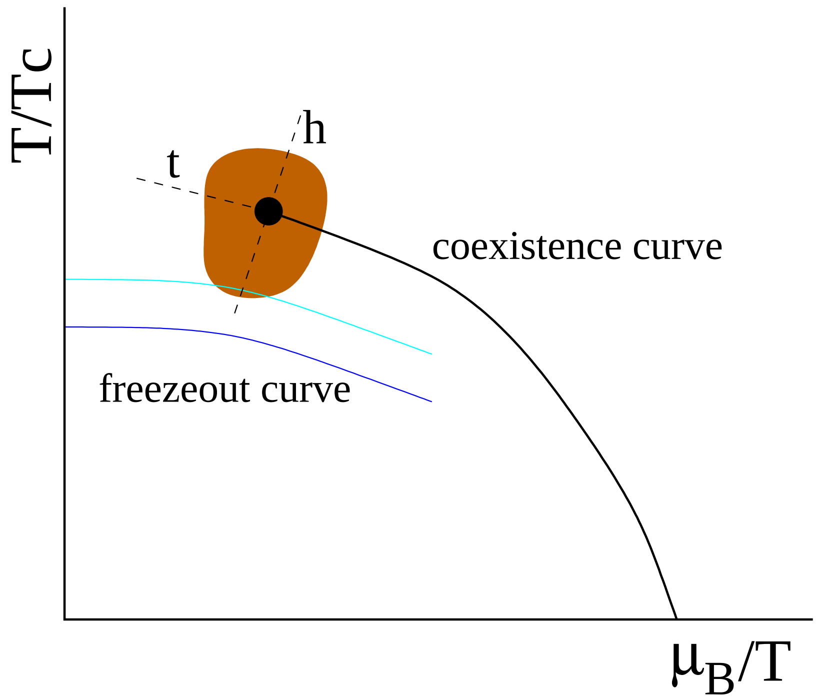
T/Tc
h
t
coexistence curve
freezeout curve
μ_B/T

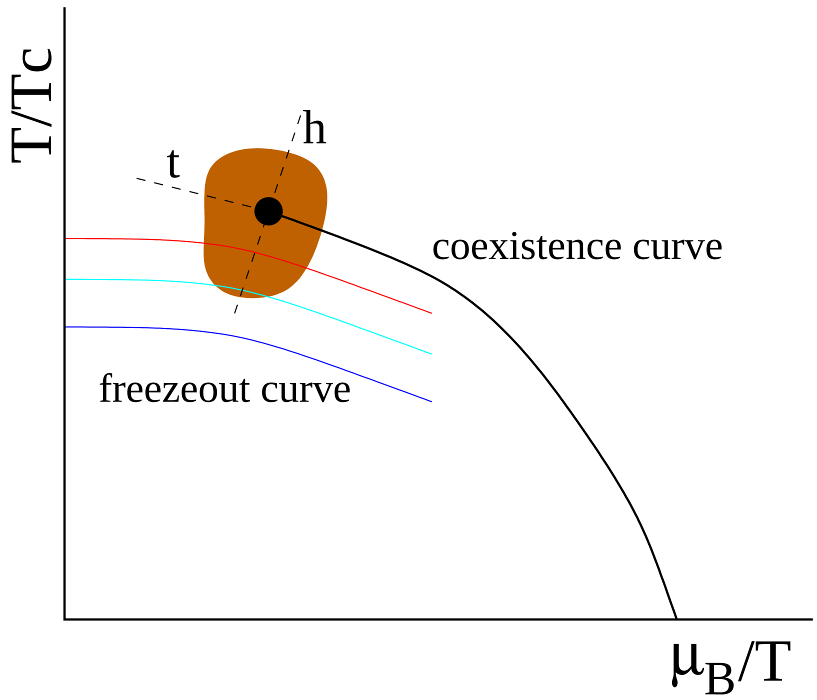

T/Tc
h
t
coexistence curve
freezeout curve
μ_B/T

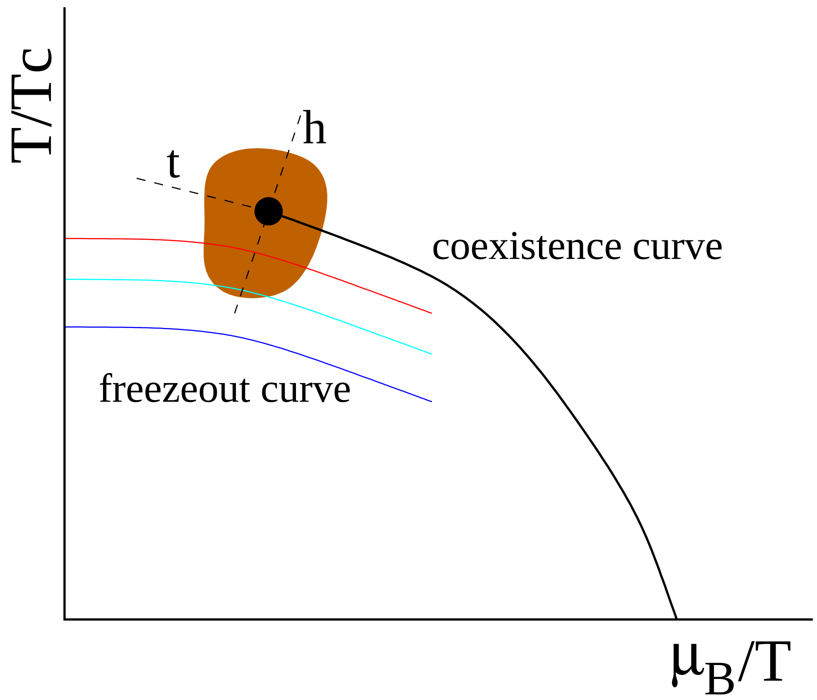

- Use the freezeout curve to relate $(T, \mu_B)$to $\sqrt{s}$ and employ lattice QCD predictions along it. (Gavai-Gupta, TIFR/TH/10-01, arXiv 1001.3796)

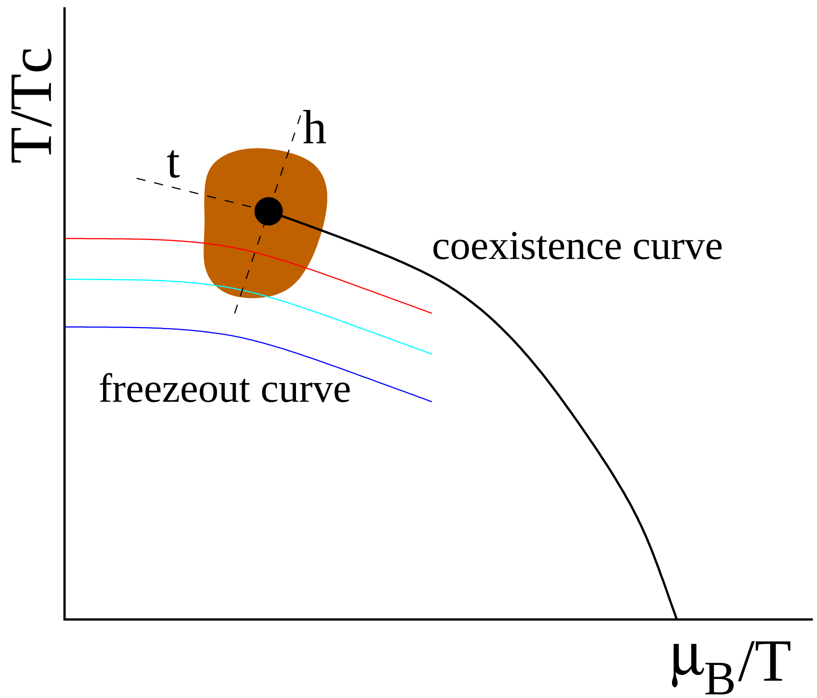

- Use the freezeout curve to relate $(T, \mu_B)$to $\sqrt{s}$ and employ lattice QCD predictions along it. (Gavai-Gupta, TIFR/TH/10-01, arXiv 1001.3796)

- Define $m_1 = \frac{T\chi^{(3)}(T,\mu_B)}{\chi^{(2)}(T,\mu_B)}$, $m_3 = \frac{T\chi^{(4)}(T,\mu_B)}{\chi^{(3)}(T,\mu_B)}$, and $m_2 = m_1 m_3$ and use the Padè method to construct them.

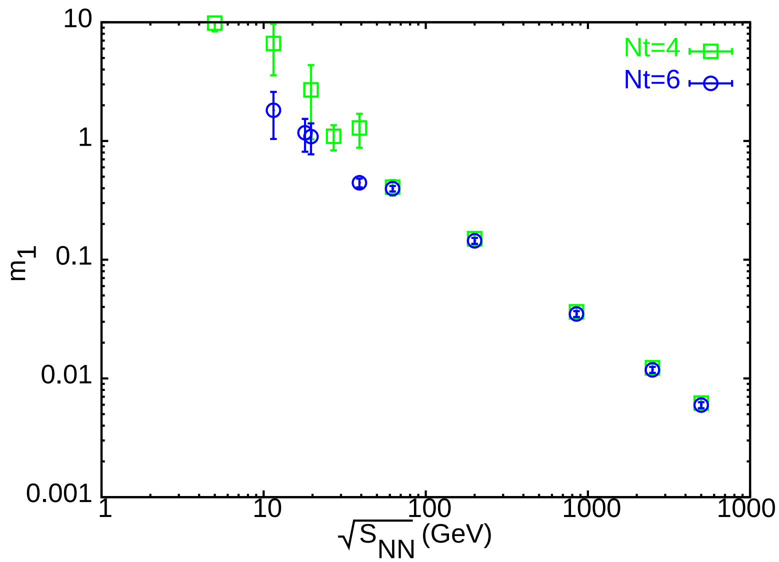

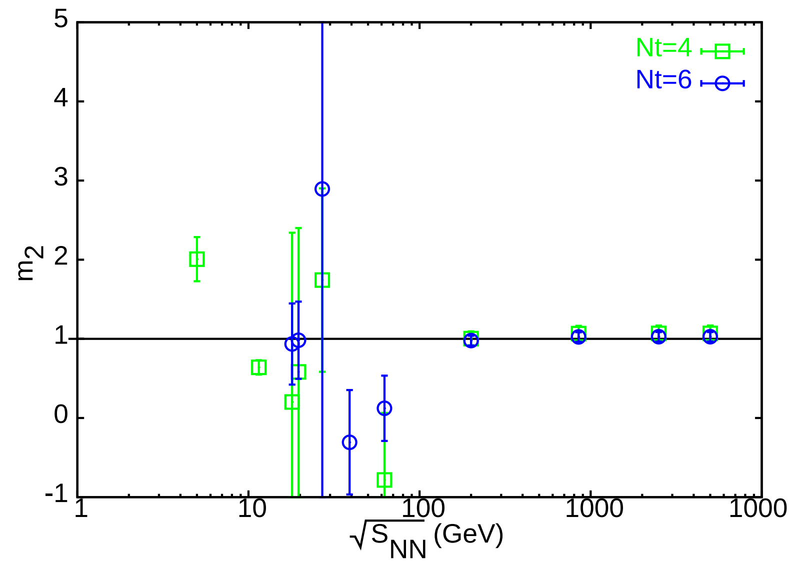

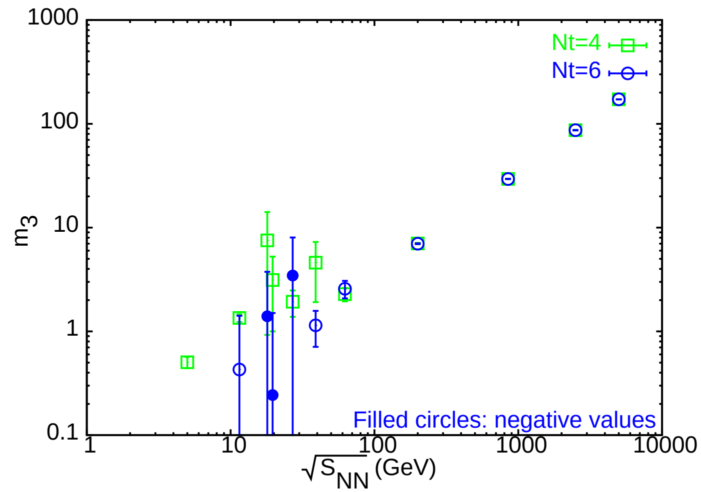

♠ Gavai & Gupta, arXiv: 1001.3796.

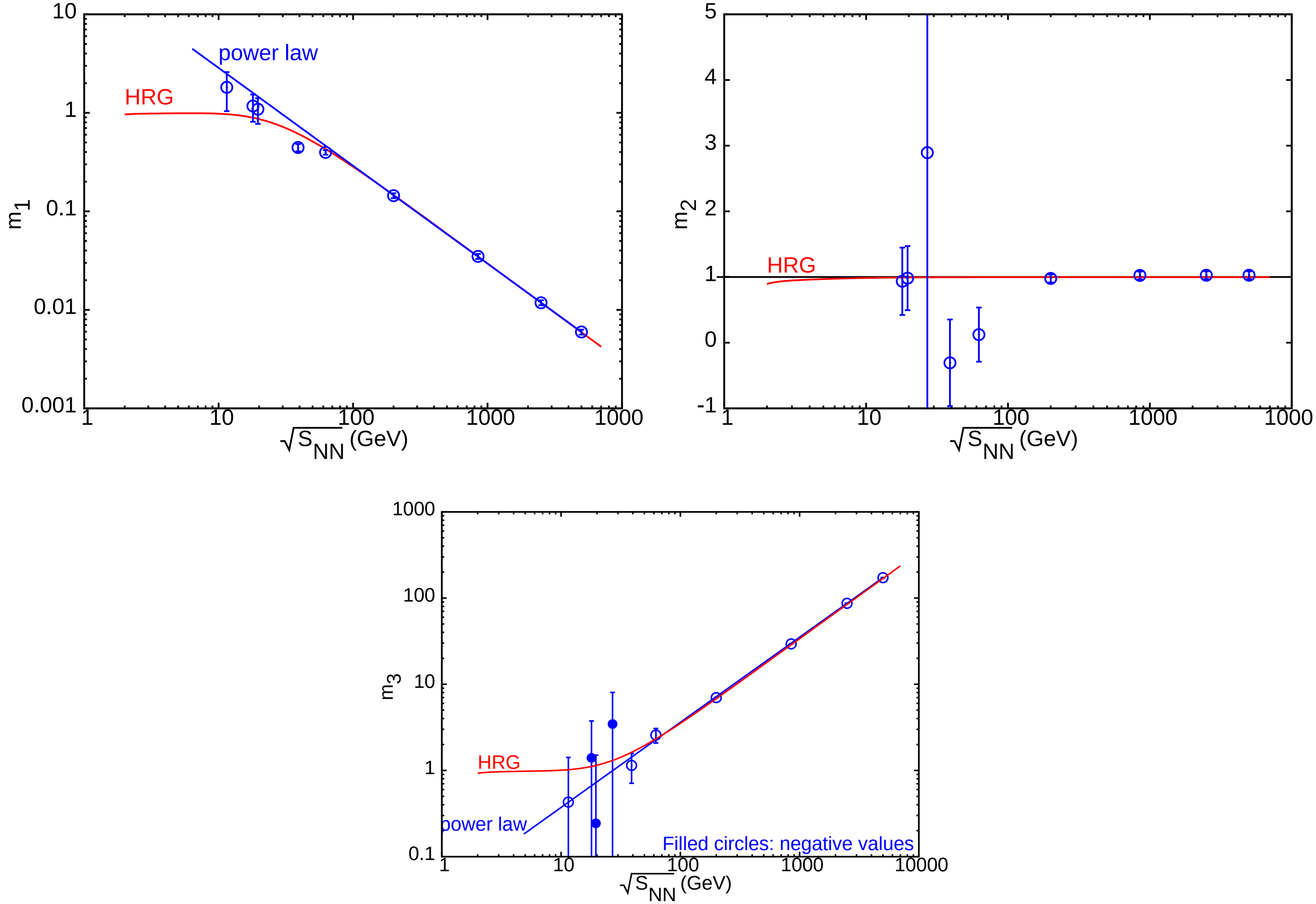

♠ Used $T_c(\mu = 0) = 170$ MeV (Gavai & Gupta, arXiv: 1001.3796).

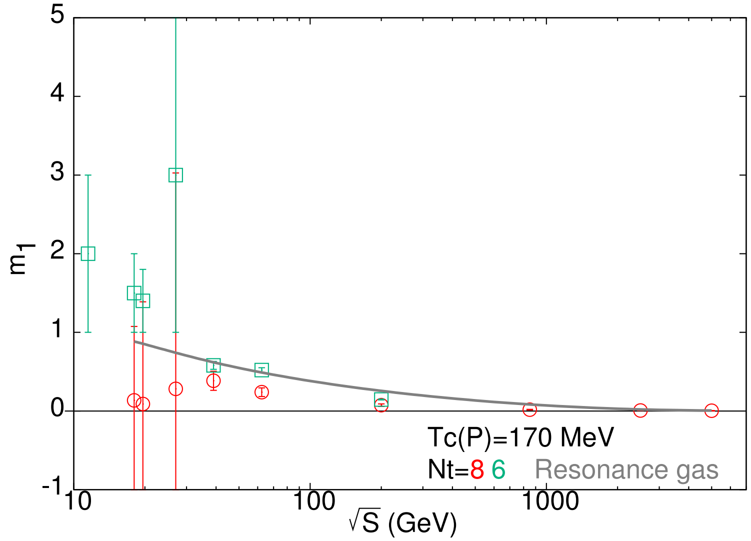

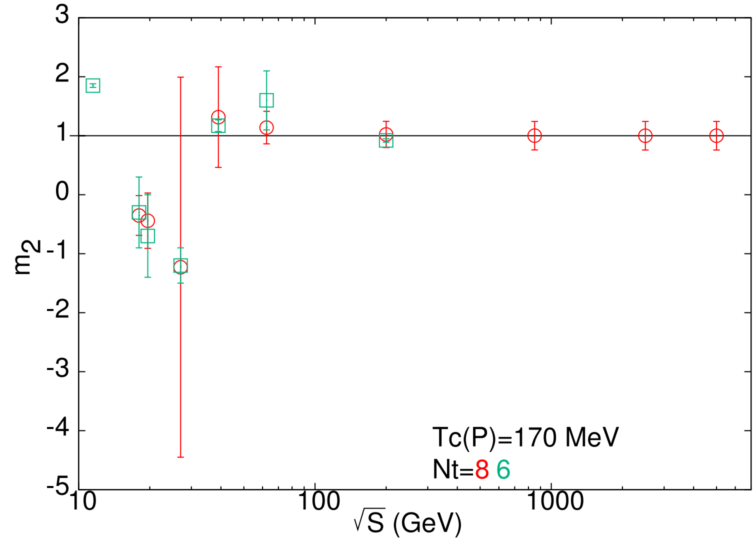

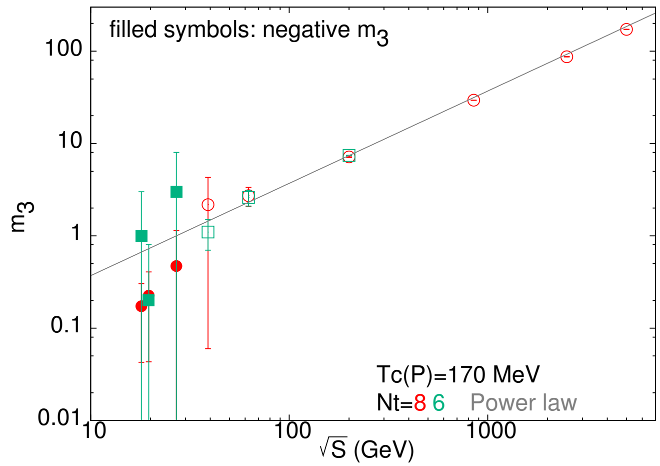

♠ Marginal change if $T_c = 175$ MeV (Datta, Gavai & Gupta, QM '12).

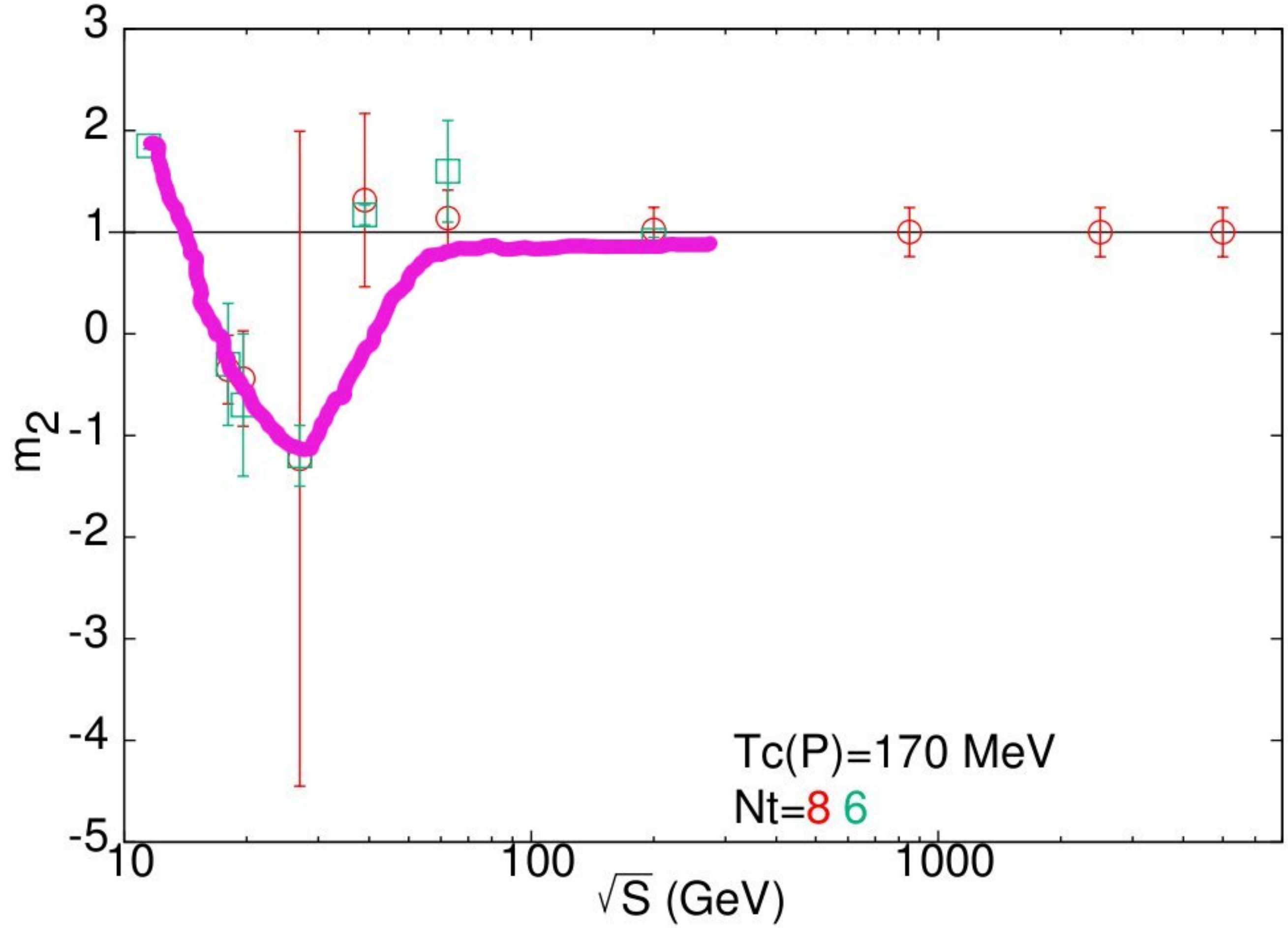

Gavai-Gupta, '10 & Datta-Gavai-Gupta, QM '12

- Smooth & monotonic behaviour for large $\sqrt{s}$: $m_1 \downarrow$ and $m_3 \uparrow$.
- Note that even in this smooth region, an experimental comparison is exciting : Direct Non-Perturbative test of QCD in hot and dense environment.

- Smooth & monotonic behaviour for large $\sqrt{s}$: $m_1 \downarrow$ and $m_3 \uparrow$.

- Note that even in this smooth region, an experimental comparison is exciting : Direct Non-Perturbative test of QCD in hot and dense environment.

- Our estimated critical point suggests non-monotonic behaviour in all m_i, which should be accessible to the low energy scan of RHIC BNL !

- Smooth & monotonic behaviour for large $\sqrt{s}$: $m_1 \downarrow$ and $m_3 \uparrow$.

- Note that even in this smooth region, an experimental comparison is exciting : Direct Non-Perturbative test of QCD in hot and dense environment.

- Our estimated critical point suggests non-monotonic behaviour in all m_i, which should be accessible to the low energy scan of RHIC BNL !

- Proton number fluctuations (Hatta-Stephenov, PRL 2003)

- Neat idea : directly linked to the baryonic susceptibility which ought to diverge at the critical point. Since diverging ξ is linked to σ mode, which cannot mix with any isospin modes, expect χ_I to be regular.

- Smooth & monotonic behaviour for large $\sqrt{s}$: $m_1 \downarrow$ and $m_3 \uparrow$.
- Note that even in this smooth region, an experimental comparison is exciting : Direct Non-Perturbative test of QCD in hot and dense environment.
- Our estimated critical point suggests non-monotonic behaviour in all m_i, which should be accessible to the low energy scan of RHIC BNL !
- Proton number fluctuations (Hatta-Stephenov, PRL 2003)
- Neat idea : directly linked to the baryonic susceptibility which ought to diverge at the critical point. Since diverging ξ is linked to σ mode, which cannot mix with any isospin modes, expect χ_I to be regular.
- Leads to a ratio χ_Q:χ_I:χ_B = 1:0:4
- Assuming protons, neutrons, pions to dominate, both χ_Q and χ_B can be shown to be proton number fluctuations only.

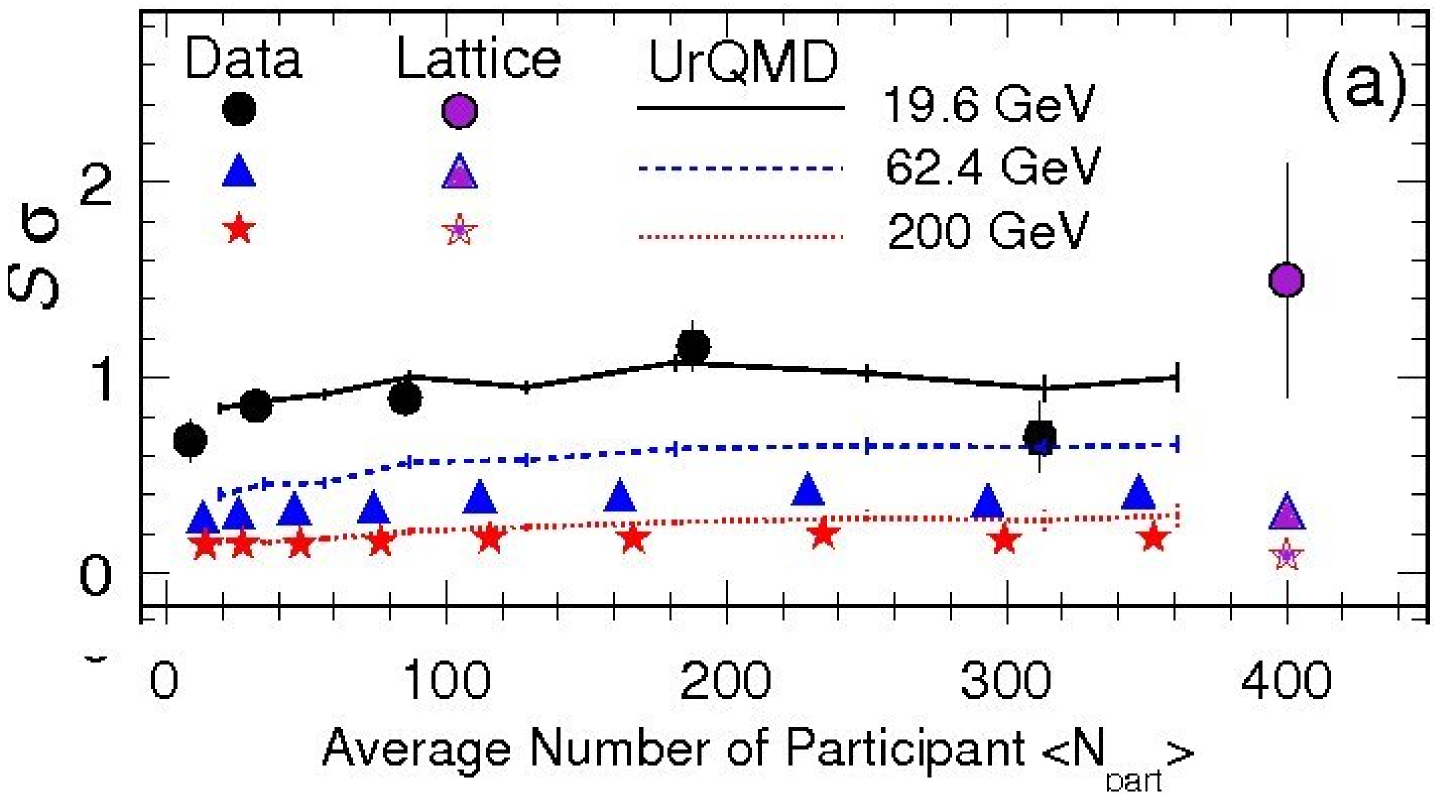

Aggarwal et al., STAR Collaboration, arXiv : 1004.4959

- Reasonable agreement with our lattice results. Where is the critical point ?

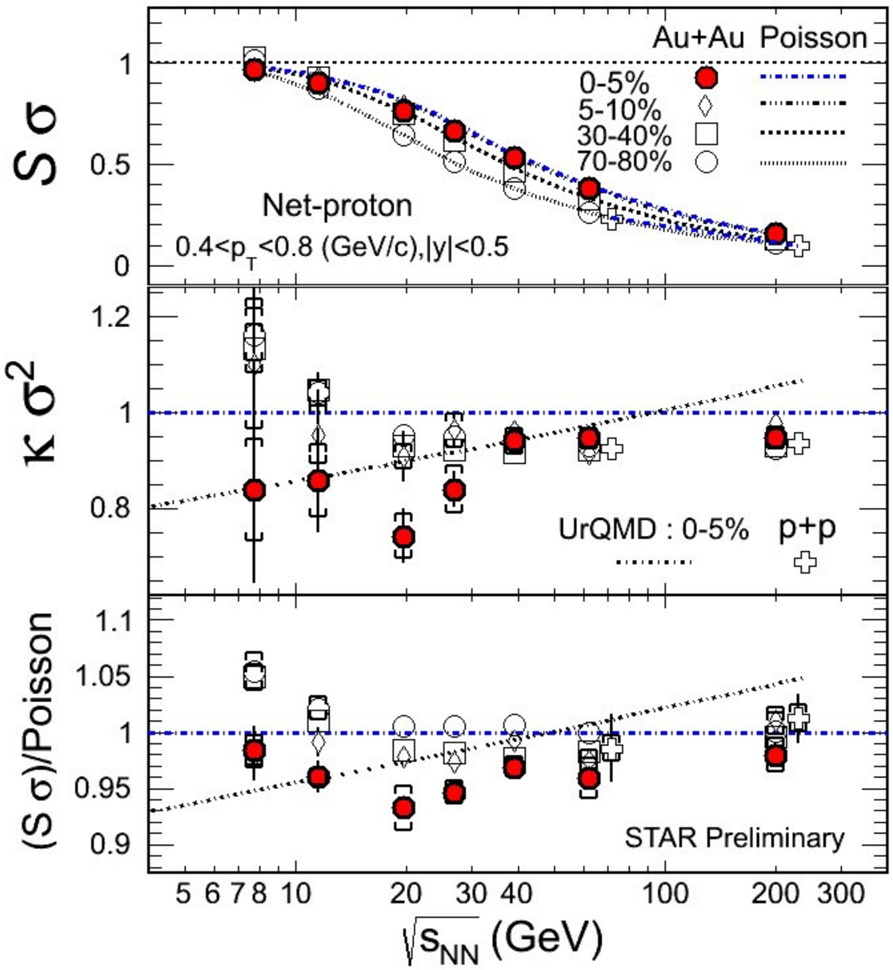

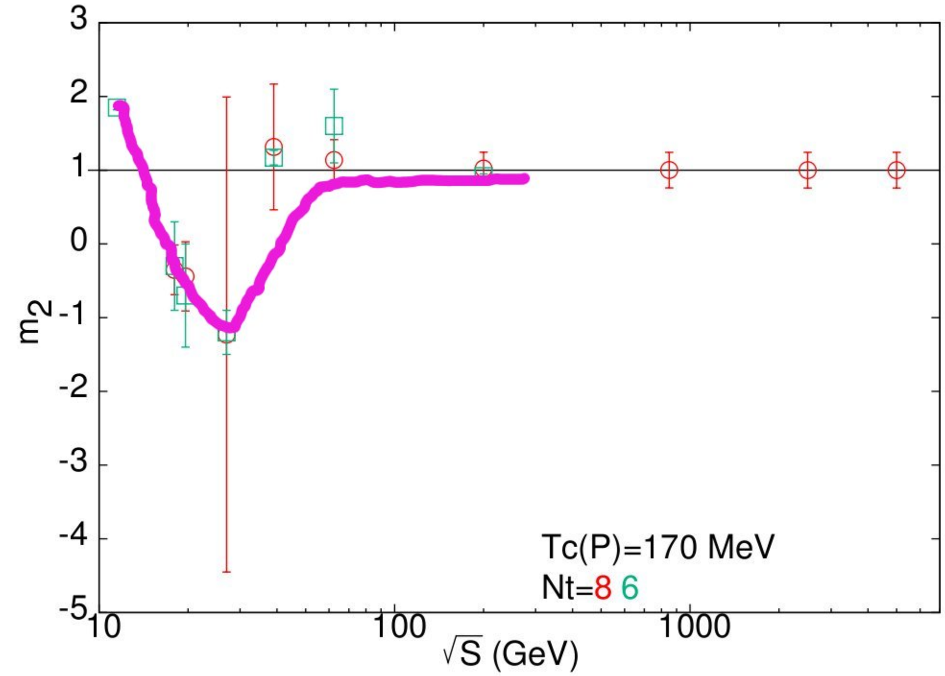

Xiaofeng Luo, QM'12
From STAR Collaboration

Gavai-Gupta, '10
Datta-Gavai-Gupta, QM '12

Summary

- Phase diagram in $T - \mu$ has begun to emerge: Different methods, $\rightsquigarrow$ similar qualitative picture. Critical Point at $\mu_B/T \sim 1 - 2$.

- Our results for $N_t = 8$ first to begin the inching towards continuum limit.

Summary

- Phase diagram in $T - \mu$ has begun to emerge: Different methods, $\rightsquigarrow$ similar qualitative picture. Critical Point at $\mu_B/T \sim 1 - 2$.

- Our results for $N_t = 8$ first to begin the inching towards continuum limit.

- We showed that Critical Point leads to structures in m_i on the Freeze-Out Curve. Possible Signatue ?

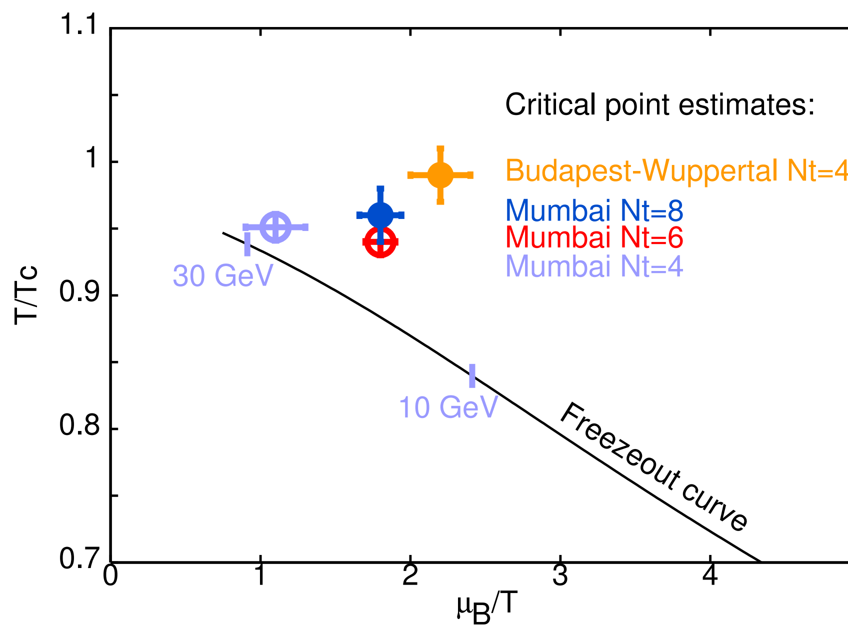

♡ STAR results appear to agree with our Lattice QCD predictions. 🙂

Lattice QCD Results

- QCD defined on a space time lattice – Best and Most Reliable way to extract non-perturbative physics: Notable successes are hadron masses & decay constants.

- The Transition Temperature T_c, the Equation of State, Heavy flavour diffusion coefficient D, Flavour Correlations C_{BS} and the Wróblewski Parameter λ_s are some examples for Heavy Ion Physics.

Lattice QCD Results

- QCD defined on a space time lattice – Best and Most Reliable way to extract non-perturbative physics: Notable successes are hadron masses & decay constants.

- The Transition Temperature T_c, the Equation of State, Heavy flavour diffusion coefficient D, Flavour Correlations C_{BS} and the Wróblewski Parameter λ_s are some examples for Heavy Ion Physics.

- Mostly staggered quarks used in these simulations. Broken flavour and spin symmetry on lattice: Less Chiral Symmetry than in continuum QCD.

Lattice QCD Results

- QCD defined on a space time lattice – Best and Most Reliable way to extract non-perturbative physics: Notable successes are hadron masses & decay constants.

- The Transition Temperature T_c, the Equation of State, Heavy flavour diffusion coefficient D, Flavour Correlations C_{BS} and the Wróblewski Parameter λ_s are some examples for Heavy Ion Physics.

- Mostly staggered quarks used in these simulations. Broken flavour and spin symmetry on lattice: Less Chiral Symmetry than in continuum QCD.

- Domain Wall or Overlap Fermions better. Computationally expensive and introduction of μ without breaking chiral symmetry needs care(Banerjee, Gavai & Sharma PRD 2008) but can be done(Gavai & Sharma PLB 2012; Narayanan-Sharma JHEP '11).

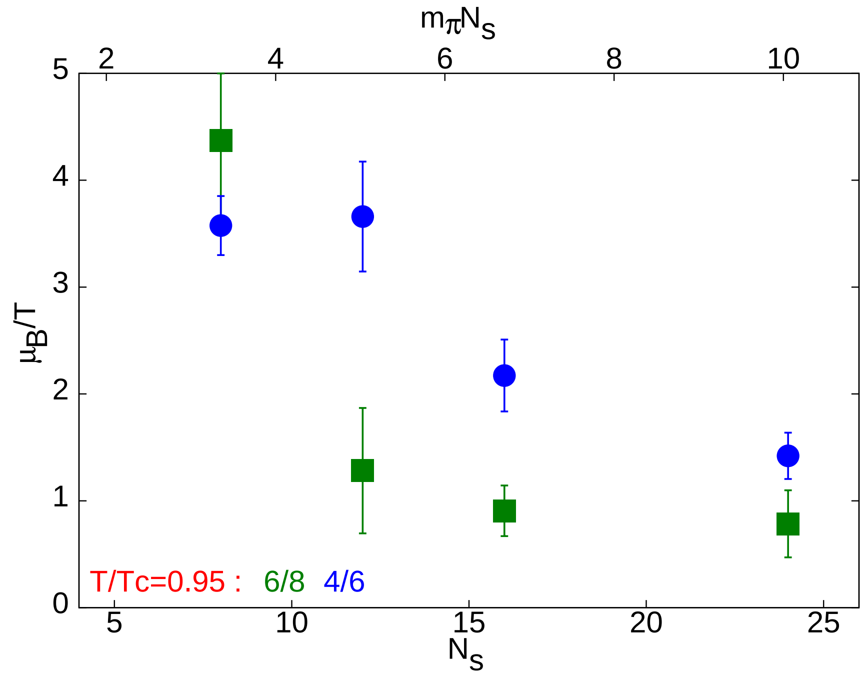

- Our estimate consistent with Fodor & Katz (2002) [$m_\pi/m_\rho = 0.31$ and $N_s m_\pi \sim$ 3-4].

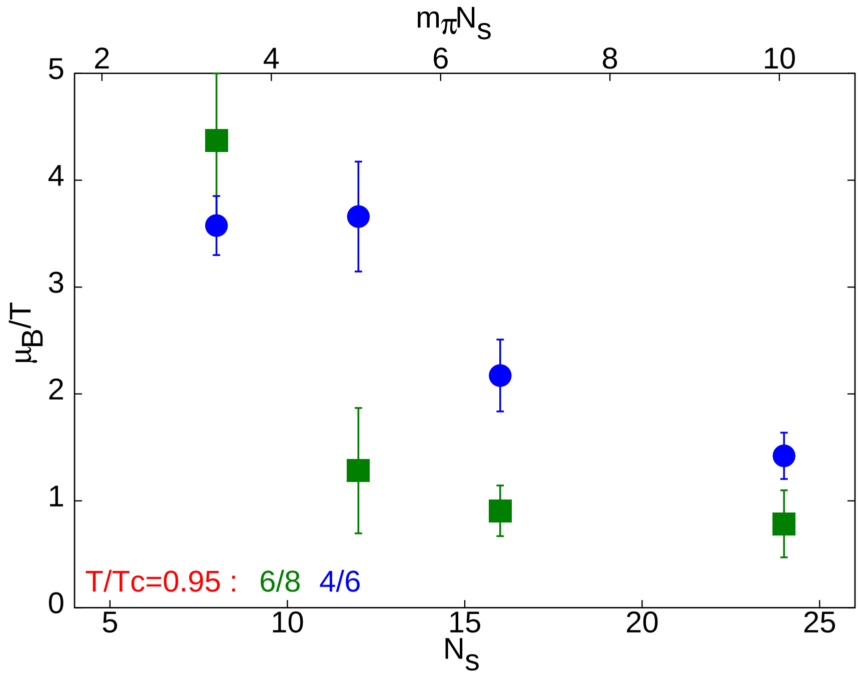

- Our estimate consistent with Fodor & Katz (2002) [$m_\pi/m_\rho = 0.31$ and $N_s m_\pi \sim$ 3-4].

- Strong finite size effects for small N_s. A strong change around $N_s m_\pi \sim 6$. (Compatible with arguments of Smilga & Leutwyler and also seen for hadron masses by Gupta & Ray)

Estimating $T_c(\mu_c)$ and μ_c/T

Status of the RBC-BI project

- calculations for $N_\tau = 4$ and 6; $N_\sigma = 4N_\tau$
- uses an $\mathcal{O}(a^2)$ improved staggered action (p4fat3)
- estimator for μ_c: $$\left(\frac{\mu_c(T)}{T_c(0)}\right)_n \equiv \rho_n = \frac{T}{T_c(0)}\sqrt{\frac{c_n}{c_{n+2}}}$$

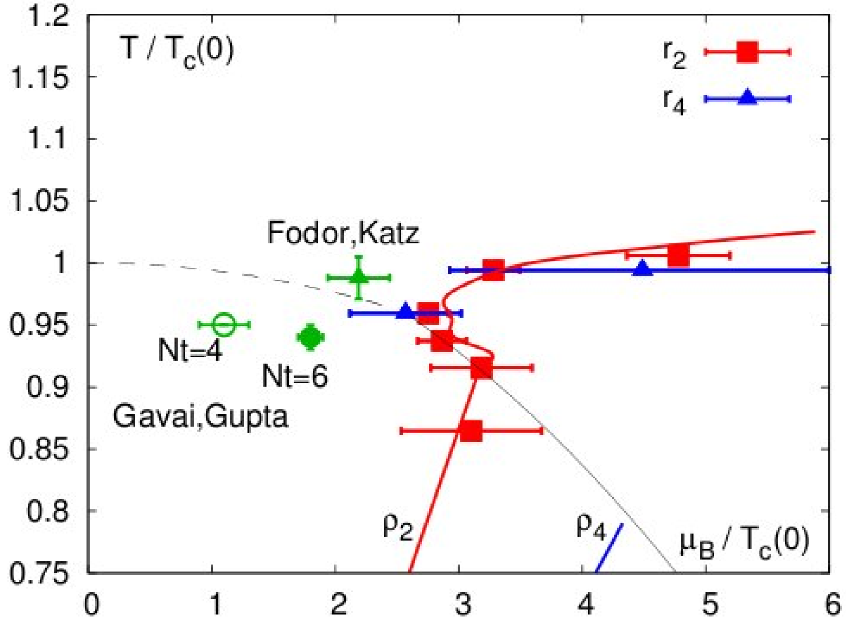

- slight quark mass dependence
- weak cut-off dependence
- $\mathcal{O}(\mu^6)$ requires more statistics

INT. Seattle 2008. F. Karsch – p. 20/3

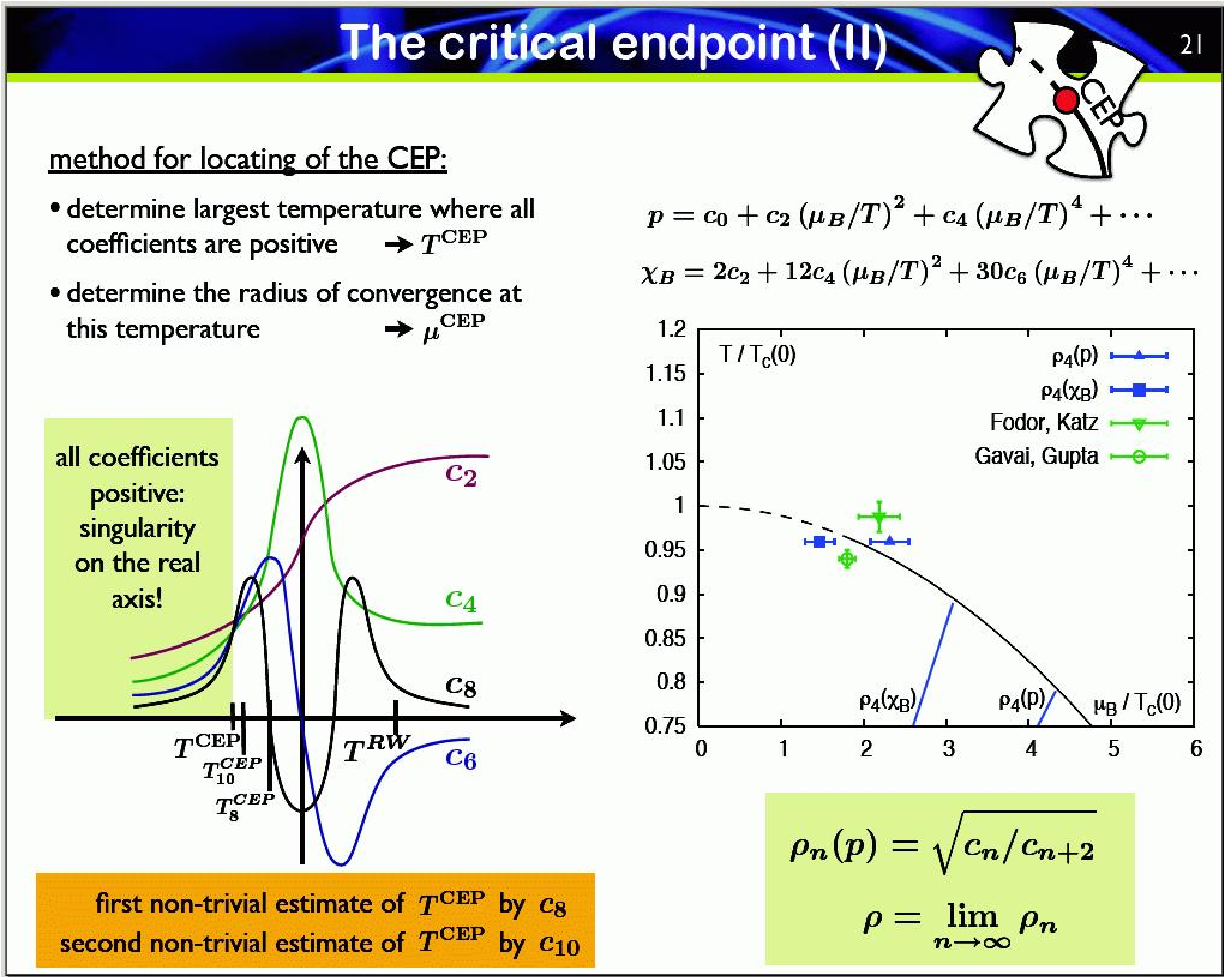

(Ch. Schmidt FAIR Lattice QCD Days, Nov 23-24, 2009.)

Imaginary Chemical Potential

deForcrand-Philpsen JHEP 0811

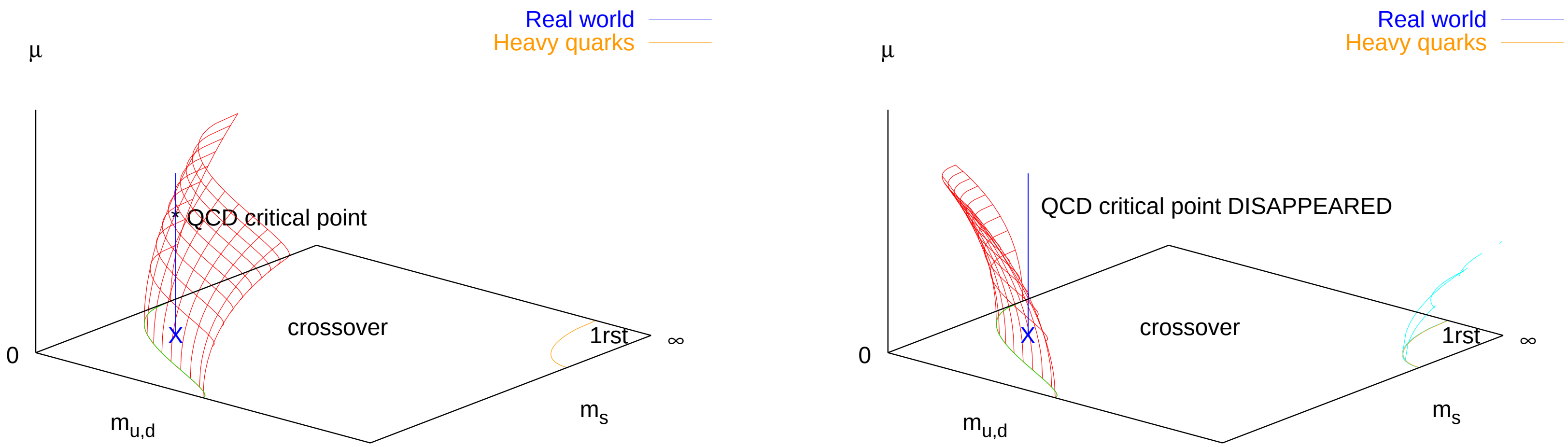

For $N_f = 3$, they find $\frac{m_c(\mu)}{m_c(0)} = 1 - 3.3(3)\left(\frac{\mu}{\pi T_c}\right)^2 - 47(20)\left(\frac{\mu}{\pi T_c}\right)^4$, i.e., m_c shrinks with μ.

Imaginary Chemical Potential

deForcrand-Philpsen JHEP 0811

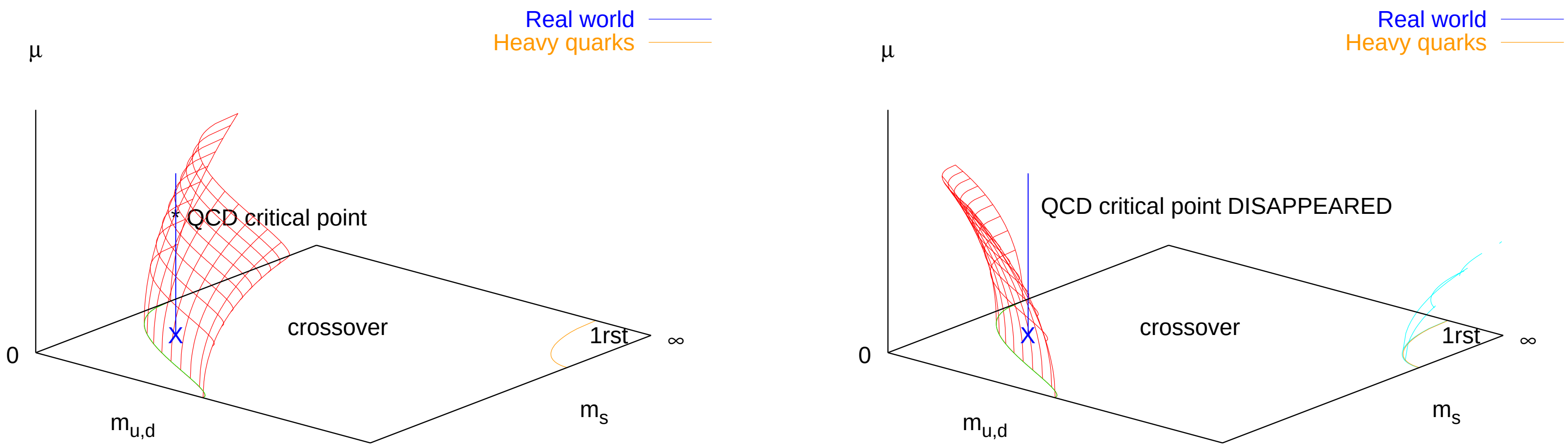

For $N_f = 3$, they find $\frac{m_c(\mu)}{m_c(0)} = 1 - 3.3(3)\left(\frac{\mu}{\pi T_c}\right)^2 - 47(20)\left(\frac{\mu}{\pi T_c}\right)^4$, i.e., m_c shrinks with μ.

Problems : i) Positive coefficient for finer lattice (Philipsen, CPOD 2009), ii) Known examples where shapes are different in real/imaginary μ, “The Critical line from imaginary to real baryonic chemical potentials in two-color QCD”, P. Cea, L. Cosmai, M. D’Elia, A. Papa, PR D77, 2008